

# New Insight into the Central Benzodiazepine Receptor—Ligand Interactions: Design, Synthesis, Biological Evaluation, and Molecular Modeling of 3-Substituted 6-Phenyl-4*H*-imidazo[1,5-*a*]-[1,4]benzodiazepines and Related Compounds<sup>†</sup>

Maurizio Anzini,<sup>\*,‡</sup> Salvatore Valenti,<sup>‡</sup> Carlo Braile,<sup>‡</sup> Andrea Cappelli,<sup>\*,‡</sup> Salvatore Vomero,<sup>‡</sup> Stefano Alcaro,<sup>§</sup> Francesco Ortuso,<sup>§</sup> Luciana Marinelli,<sup>||</sup> Vittorio Limongelli,<sup>||</sup> Ettore Novellino,<sup>||</sup> Laura Betti,<sup>⊥</sup> Gino Giannaccini,<sup>⊥</sup> Antonio Lucacchini,<sup>⊥</sup> Simona Daniele,<sup>⊥</sup> Claudia Martini,<sup>⊥</sup> Carla Ghelardini,<sup>#</sup> Lorenzo Di Cesare Mannelli,<sup>#</sup> Gianluca Giorgi,<sup>∞</sup> Maria Paola Mascia,<sup>●,▼</sup> and Giovanni Biggio<sup>●,▼</sup>

<sup>†</sup>Dipartimento Farmaco Chimico Tecnologico and European Research Centre for Drug Discovery and Development, Università degli Studi di Siena, Via A. Moro, 53100 Siena, Italy

<sup>§</sup>Dipartimento di Scienze Farmacobiologiche, Università “Magna Græcia” di Catanzaro, Complesso Nini Barbieri, 88021 Roccelletta di Borgia (CZ), Italy

<sup>||</sup>Dipartimento di Chimica Farmaceutica e Tossicologica, Università di Napoli “Federico II”, Via D. Montesano 49, 80131 Napoli, Italy

<sup>⊥</sup>Dipartimento di Psichiatria, Neurobiologia Farmacologia e Biotecnologie, Università di Pisa, Via Bonanno 6, 56126 Pisa, Italy

<sup>#</sup>Dipartimento di Farmacologia Preclinica e Clinica “M. Aiazzi Mancini”, Università degli Studi di Firenze, Viale G. Pieraccini 6, 50139 Firenze, Italy

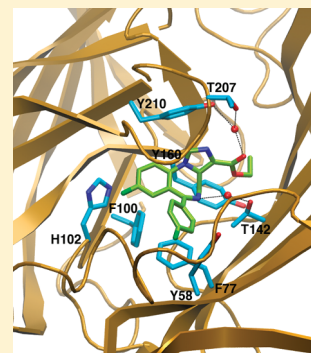
<sup>∞</sup>Dipartimento di Chimica, Università degli Studi di Siena, Via A. Moro, 53100 Siena, Italy

<sup>●</sup>Dipartimento di Biologia Sperimentale “B. Loddo”, Sezione Neuroscienze, Università degli Studi di Cagliari, Cittadella Universitaria, S.S. 554, Km. 4.500, 09042 Monserrato (CA), Italy

<sup>▼</sup>Istituto di Neuroscienze, Consiglio Nazionale delle Ricerche, Cittadella Universitaria, S.S. 554, Km 4.500, 09042 Monserrato (CA), Italy

## **S** Supporting Information

**ABSTRACT:** 3-Substituted 6-phenyl-4*H*-imidazo[1,5-*a*][1,4]benzodiazepines and related compounds were synthesized as central benzodiazepine receptor (CBR) ligands. Most of the compounds showed high affinity for bovine and human CBR, their  $K_i$  values spanning from the low nanomolar to the submicromolar range. In particular, imidazoester **5f** was able to promote a massive flow of  $^{36}\text{Cl}^-$  in rat cerebrocortical synaptoneurosomes overlapping its efficacy profile with that of a typical full agonist. Compound **5f** was then examined in mice for its pharmacological effects where it proved to be a safe anxiolytic agent devoid of the unpleasant myorelaxant and amnesic effects of the classical 1,4-benzodiazepines. Moreover, the selectivity of some selected compounds has been assessed in recombinant  $\alpha_1\beta_2\gamma_2\text{L}$ ,  $\alpha_2\beta_1\gamma_2\text{L}$ , and  $\alpha_5\beta_2\gamma_2\text{L}$  human GABA<sub>A</sub> receptors. Finally, some compounds were submitted to molecular docking calculations along with molecular dynamics simulations in the Cromer’s GABA<sub>A</sub> homology model.



## **■ INTRODUCTION**

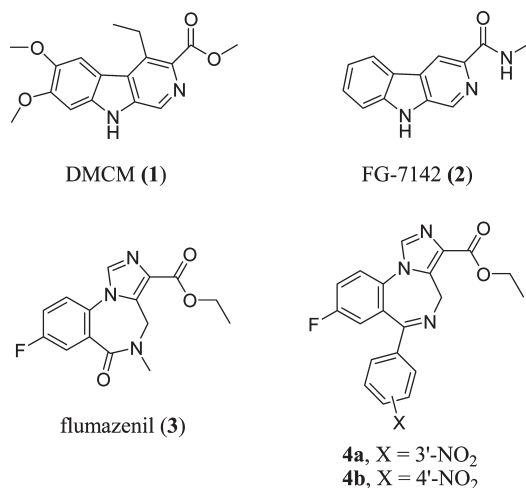
The action of  $\gamma$ -aminobutyric acid (GABA) on the GABA<sub>A</sub> chloride channel complex is capable of controlling the excitability of many central nervous system (CNS) pathways, and it is estimated that over 20–50% of all central synapses utilize GABA as their transmitter, depending on the brain region.<sup>1</sup> GABA<sub>A</sub> receptors are ligand-gated chloride ion channels that contain allosteric sites in addition to the agonist binding site, through which other agents can modulate receptor function.<sup>2</sup> Positive modulators of the GABA<sub>A</sub> receptors, such as the classical 1,4-benzodiazepines [BDZ, e.g., diazepam (7-chloro-1,3-dihydro-1-methyl-5-phenyl-2*H*-1,4-benzodiazepin-2-one), lorazepam (7-chloro-5-(*o*-chlorophenyl)-1,3-dihydro-3-hydroxy-2*H*-1,4-benzodiazepin-2-one)], the neuroactive steroids [e.g., pregnenolone

(3 $\beta$ -hydroxypregn-5-ene-20-one), allopregnenolone (3 $\beta$ -hydroxy-5 $\alpha$ -pregn-16-en-20-one)], and the barbiturates [e.g., pentobarbital (5-ethyl-5-(1-methylbutyl)barbituric acid)], are prescribed as sedatives, muscle relaxants, anxiolytics, and anticonvulsants. Conversely, negative GABA<sub>A</sub> modulators, such as BDZ inverse agonists [e.g.,  $\beta$ -carboline DMCM (**1**) and FG-7142 (**2**), Chart 1] and the neuroactive steroids [e.g., pregnenolone sulfate, dehydroepiandrosterone sulfate (3 $\beta$ -hydroxyandrost-5-en-17-one)], have anxiogenic and convulsant effects.<sup>3–6</sup> Neutral modulators such as the central benzodiazepine receptor (CBR) antagonist flumazenil (**3**) (ethyl

**Received:** February 11, 2011

**Published:** July 14, 2011

Chart 1. Structures of Reference Compounds



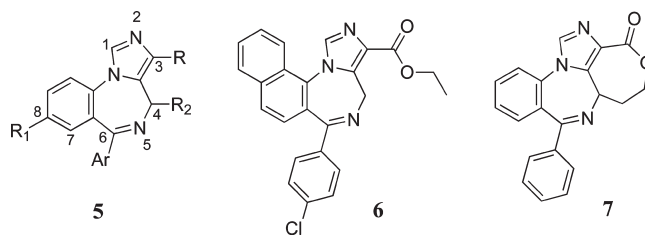
8-fluoro-5,6-dihydro-5-methyl-6-oxo-4*H*-imidazo[1,5-*a*][1,4]-benzodiazepine-3-carboxylate) (Chart 1) bind to GABA<sub>A</sub> receptor but have no intrinsic activity, although flumazenil antagonizes the effects of both positive and negative GABA<sub>A</sub> modulators that act via the CBR.

Positive GABA<sub>A</sub> modulators are useful in inducing not only sedation and muscle relaxation prior to surgical procedures but also amnesia.<sup>7</sup> The amnesic effects of the positive modulators in animal and man are well established,<sup>8–10</sup> and thus, it has been hypothesized that the negative modulators being procognitive<sup>11,12</sup> may have the opposite effect. Indeed improvements in learning and memory dysfunction have been reported after dehydroepiandrosterone administration to individuals with low dehydroepiandrosterone sulfate levels,<sup>13</sup> but further studies have failed to demonstrate a significant effect of these steroids on cognitive abilities.<sup>14,15</sup> Thus, the therapeutic use of neurosteroids for cognitive dysfunction is of uncertain value.<sup>16</sup> Similarly, non-selective BDZ inverse agonists cannot be used to treat neurological disorders associated with cognitive impairment because of their profound anxiogenic and proconvulsant liabilities.<sup>17</sup> The discrete localization of the different BDZ-sensitive GABA<sub>A</sub> receptors subtypes provides restricted targets within the brain, potentially offering improvement in the therapeutic window for negative GABA<sub>A</sub> receptors modulators.

At present, a total of 21 subunits ( $\alpha_{1-6}$ ,  $\beta_{1-4}$ ,  $\gamma_{1-4}$ ,  $\delta$ ,  $\epsilon$ ,  $\pi$ ,  $\theta$ , and  $\rho_{1-3}$ ) have been cloned and sequenced with the majority of GABA<sub>A</sub> receptors comprising of  $\alpha$ ,  $\beta$ , and  $\gamma$  subunits arranged in a 2:2:1 stoichiometry. The subunits may theoretically coassemble to form a plethora of structurally different ion pores, but among the multitude of possible receptor subtype combinations, only those that contain a  $\gamma_2$  or  $\gamma_3$ <sup>18</sup> subunit in conjunction with  $\alpha_1$ ,  $\alpha_2$ ,  $\alpha_3$ , or  $\alpha_5$  seem to bind BDZ ligands with significant affinity. In particular, BDZ pharmacological effects are strictly related to the  $\alpha$  isoform.<sup>19</sup>

The benzodiazepine binding pocket appears to be located at the interface of  $\gamma$  and  $\alpha$  subunits, with the residues on both proteins making significant contributions to the active site. Since the GABA binding site requires contributions from both an  $\alpha$  and  $\beta$  subunit, we therefore need only consider channels composed of  $\alpha$ ,  $\beta$ , and  $\gamma$  subtypes for our purposes.<sup>20</sup>

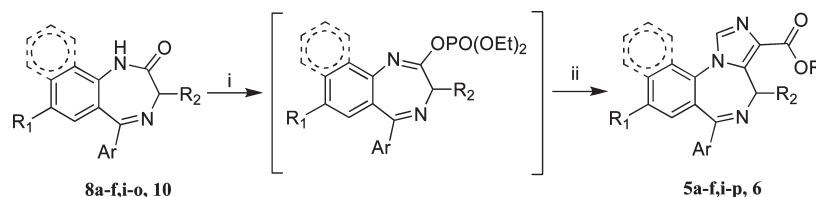
Studies using molecular genetic or pharmacological approaches have indicated that GABA<sub>A</sub> receptors containing an  $\alpha_1$  subunit

Chart 2. Structures of 3-Substituted 6-Phenyl-4*H*-imidazo[1,5-*a*][1,4]benzodiazepines 5 and Related Compounds 6 and 7

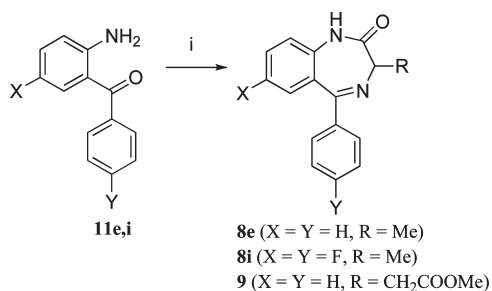
account for the sedative and muscle relaxant effects of non-selective BDZ agonists, whereas those with an  $\alpha_2$  or  $\alpha_3$  subunit mediate the anxiolytic and anticonvulsant effects.<sup>21–23</sup>

In situ hybridization and immunocytochemistry studies have shown that the  $\alpha_5$  GABA<sub>A</sub> receptor subtype is preferentially expressed at high levels in the hippocampus, although it is also found to a lesser degree within the cortex and the olfactory bulb.<sup>24,25</sup> The receptors are thought to be located extrasynaptically<sup>26</sup> and play a role in tonic inhibition of hippocampal CA1 pyramidal neurons.<sup>27</sup> Furthermore, the hippocampal  $\alpha_5$ -mediated tonic conductance is highly sensitive to anesthetics, which are known to produce a pronounced amnesic effect in vivo.<sup>28</sup> Although many regions of the CNS are involved in cognitive functions, the hippocampus clearly plays a key role.<sup>29</sup> It has been suggested that BDZ agonists may exert their amnesic effects by modulating hippocampal function, since the anterograde rather than retrograde amnesia is similar to deficits induced by hippocampal lesions in animals and man.<sup>30</sup> It has therefore been hypothesized<sup>11,31</sup> that  $\alpha_5$  subtype-selective inverse agonists could be procognitive but devoid of anxiogenic and proconvulsant effects associated with activity at other GABA<sub>A</sub> receptor subtypes. Up to now, only modest progress has been made in the design of receptor-subtype selective ligands, although numerous papers detailing success in achieving selectivity in the synthesis of BDZ ligands that exhibit 100-fold selectivity toward particular GABA receptor isoforms have been published.<sup>32–35</sup> Unfortunately, as Harris et al. stated in a very recent paper: “BDZ ligands that exhibit true specificity to a single GABA<sub>A</sub> receptor isoform (affinities 1000-fold higher for one GABA<sub>A</sub> receptor isoform over all other isoforms) are to date rare.”<sup>36</sup> Thus, within a large research project aimed at deepening the study of ligand–CBR interactions and in order to extend knowledge about our previously reported binding mode<sup>37</sup> of two imidazo[1,5-*a*][1,4]benzodiazepine esters (4a,b) (Chart 1), we focused our attention on the synthesis of a new series of 3-substituted 6-phenyl-4*H*-imidazo[1,5-*a*][1,4]-benzodiazepines (5a–u) and related compounds (6 and 7) (Chart 2), the biological activity of which was assayed in vitro and in vivo and the results of these studies were rationalized through extensive computational studies.

In particular, different halogen atoms or small substituents were introduced into the benzo ring and the pendent phenyl with the aim of modulating affinity and intrinsic activity of imidazo[1,5-*a*][1,4]benzodiazepine esters 5. Furthermore, compounds 5p–u were synthesized with the aim of probing a more hindered or a more polar side chain than carboxyethyl moiety. Naphthyl derivative 5o and naphtho-fused compound 6 were synthesized to investigate the steric tolerance in correspondence to the benzo

Scheme 1. Imidazo Annulation of Diazepinone Derivatives 8a–f,i–o and 10<sup>a</sup>

<sup>a</sup> Reagents: (i) *t*-BuOK, ClPO(OEt)<sub>2</sub>, THF; (ii) CNCH<sub>2</sub>COOEt or CNCH<sub>2</sub>COO-*t*-Bu, *t*-BuOK.

Scheme 2. Synthesis of 3-Substituted Benzodiazepin-2-one Derivatives 8e,i and 9<sup>a</sup>

<sup>a</sup> Reagents: (i) CH<sub>3</sub>CH(NH<sub>2</sub>)COOEt·HCl or MeOOCCH(NH<sub>2</sub>)·CH<sub>2</sub>COOMe·HCl, pyridine.

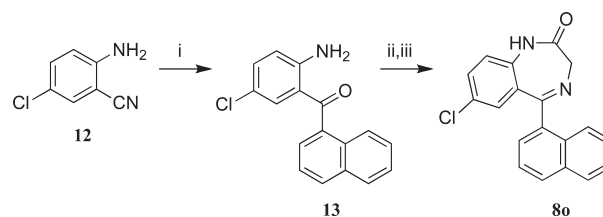
and the pendent phenyl ring, respectively. Finally, conformational constrained derivatives **5e,i** and **7** were designed in order to evaluate our hypothesis on the orientation of the carboxyethyl group with respect to the imidazo ring.<sup>37</sup>

## CHEMISTRY

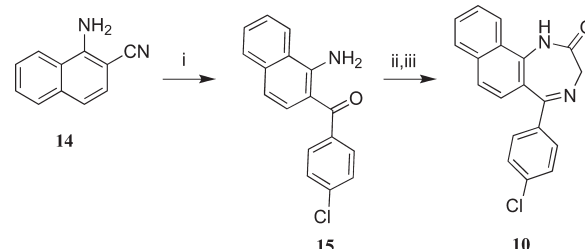
The synthesis of imidazoesters **5a–f,i–p** and **6** was carried out as depicted in Scheme 1. Briefly, the imidazo annulation of diazepinone derivatives **8a–f,i–o** and **10** was accomplished via the corresponding phosphonate intermediate by reaction with ethyl isocyanoacetate or *tert*-butyl isocyanoacetate in the presence of potassium *tert*-butoxide, providing the imidazoesters **5a–f,i–p** and **6** in satisfactory yield.<sup>38</sup>

The synthetic route used to prepare benzodiazepinones **8a–d,f,j–n** starting from the suitable 2-aminobenzophenones involved the sequential treatment with bromoacetyl bromide in dichloromethane to give the corresponding bromoacetamides and then with ammonia in ethanol at reflux or the reaction with glycine ethyl ester in pyridine at reflux.<sup>39,40</sup> On the other hand, racemic 3-substituted 1,4-benzodiazepinones **8e,i** and **9** were prepared by condensation of the suitable benzophenone derivative (**11e,i**) with alanine ethyl ester or aspartic acid dimethyl ester hydrochloride in pyridine (Scheme 2).

The synthesis of benzodiazepinone **8o** was carried out starting from 2-amino-5-chlorobenzonitrile **12**, which was treated with Grignard's reagent, 1-naphthylmagnesium bromide, in diethyl ether to afford the expected naphthyl derivative **13** (Scheme 3). Condensation of **13** with bromoacetyl bromide in dichloromethane gave the respective bromoacetamide, which was in turn cyclized into the expected lactam **8o** in the presence of liquid ammonia in methanol at reflux.

Scheme 3. Synthesis of 7-Chloro-5-naphthyl-1,4-benzodiazepinone **8o**<sup>a</sup>

<sup>a</sup> Reagents: (i) 1-bromonaphthalene, Mg, dry EtOEt; (ii) BrCH<sub>2</sub>COBr, CH<sub>2</sub>Cl<sub>2</sub>; (iii) liquid NH<sub>3</sub>, MeOH.

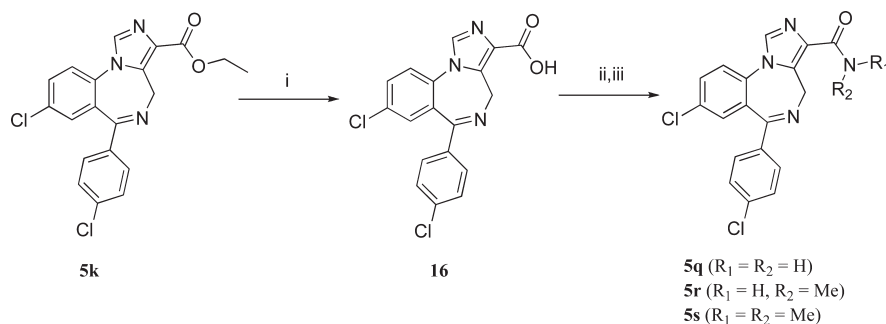
Scheme 4. Synthesis of 5-(4-Chlorophenyl)naphthodiazepinone Derivative **10**<sup>a</sup>

<sup>a</sup> Reagents: (i) 4-bromochlorobenzene, Mg, dry EtOEt; (ii) BrCH<sub>2</sub>COBr, CH<sub>2</sub>Cl<sub>2</sub>; (iii) liquid NH<sub>3</sub>, MeOH.

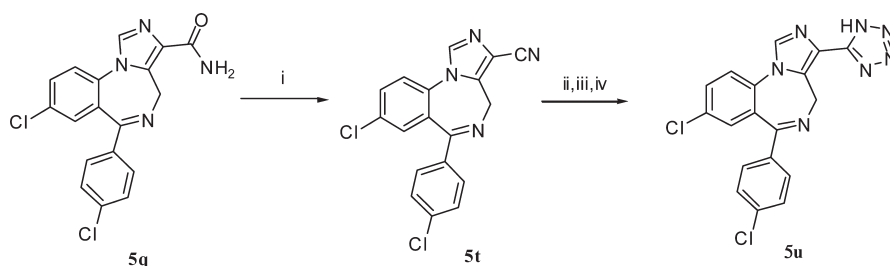
The naphtho-fused diazepinone **10** was synthesized as sketched in Scheme 4. In this sequence, the conversion of 1-amino-2-naphthonitrile **14**<sup>41</sup> into  $\alpha$ -aminonaphthophenone **15** was accomplished by treatment with Grignard's reagent, 4-chlorophenylmagnesium bromide, and the condensation of **15** with bromoacetyl bromide and successive cyclization of the bromoacetamide in the presence of liquid NH<sub>3</sub> to accomplish the ring closure as for compound **8o** afforded naphthodiazepinone **10**.

The alkaline hydrolysis of imidazo ester **5k** afforded corresponding acid **16**, which by sequential treatment with isobutyl chloroformate and the proper amine (or ammonia) was converted into expected carboxamides **5q–s** as depicted in Scheme 5.

Dehydration of amide **5q**, by means of phosphorus oxychloride in dry benzene, afforded imidazocarbonitrile **5t** in good yield, as the precursor of tetrazole derivative **5u**. Compound **5t** underwent a 1,3-dipolar cycloaddition with trimethyltin azide to give, after protection with triphenylchloromethane and deprotection with HCl, imidazotetrazole derivative **5u** (Scheme 6).

Scheme 5. Synthesis of Carboxamides 5q–s<sup>a</sup>

<sup>a</sup> Reagents: (i) 2 N NaOH, EtOH; (ii) ClCOO-*i*-Bu, TEA, CHCl<sub>3</sub>; (iii) NH<sub>3</sub> or NH<sub>2</sub>CH<sub>3</sub> or NH(CH<sub>3</sub>)<sub>2</sub>.

Scheme 6. Synthesis of 1H-Tetrazole Derivative 5u<sup>a</sup>

<sup>a</sup> Reagents: (i) POCl<sub>3</sub>, benzene; (ii) (CH<sub>3</sub>)<sub>3</sub>SnN<sub>3</sub>, xylene; (iii) 10 N NaOH, CH<sub>2</sub>Cl<sub>2</sub>, THF, and then ClC(C<sub>6</sub>H<sub>5</sub>)<sub>3</sub>; (iv) 10% HCl, THF.

The synthesis of conformationally constrained derivative 7 was achieved starting from 9, which was reduced in the presence of lithium aluminum hydride to afford the corresponding hydroxyethyl derivative 17. After the protection of the alcoholic function by means of *tert*-butylchlorodimethylsilane,<sup>42</sup> compound 18 was cyclized to the imidazo ester 19 and deprotected in the presence of (*n*-Bu)<sub>4</sub>NF to give alcohol 20 which, by treatment with sodium hydride in DMF, gave the expected imidazolactone 7 in satisfactory yield (Scheme 7).

## RESULTS AND DISCUSSION

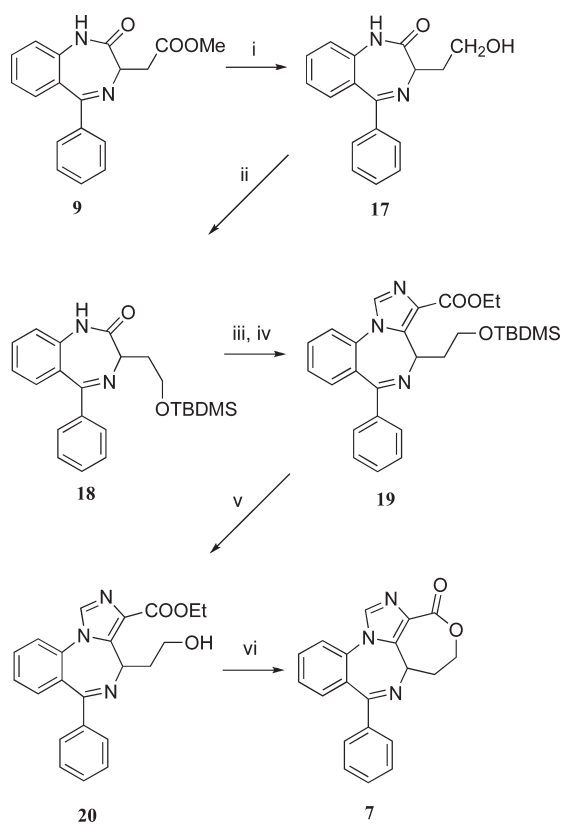
**In Vitro Binding.** The binding affinity of the imidazo[1,5-*a*]-[1,4]benzodiazepine derivatives 5a–u, 6, and 7 to the benzodiazepine receptor in bovine and human cortical membranes was determined by means of competition experiments against the radiolabeled antagonist [<sup>3</sup>H]flumazenil and expressed as K<sub>i</sub> values when the compounds inhibited radioligand binding by more than 80% at the fixed concentration of 10 μM. The in vitro efficacy of the tested compounds was measured by the GABA ratio (GR), which predicts the pharmacological profile of a CBR ligand.<sup>43–45</sup> The resulting value, expressed as a ratio of K<sub>i</sub> without GABA to K<sub>i</sub> with GABA, is nearly 2 for a full agonist and around 1 for an antagonist; partial agonists show intermediate values between 1 and 2, while a GABA ratio value below 1 is typical for inverse agonists. The data summarized in Table 1 show that most of the newly synthesized compounds interact with CBR, showing affinities from the low nanomolar to the submicromolar ranges.

The structure–affinity relationship analysis shows that substituents in positions 8 and 4' of the 6-phenylimidazo[1,5-*a*]-[1,4]benzodiazepine scaffold play a key role in modulating the

interaction at the CBR binding site. In particular, the presence of small atoms (e.g., H or F) in position 8 is required for nanomolar CBR affinity, whereas the presence of the bulkier chlorine atom produces a drop in CBR affinity that achieves about 1 order of magnitude when F, Cl, or CH<sub>3</sub> is present in the 4' position.

A particular case is represented by the 8-Cl-3'-NO<sub>2</sub> derivative 5n, which shows affinity in the low nanomolar range slightly higher than its 8-fluoro analogue 5g. This result confirms that the electronic properties of NO<sub>2</sub> group have a dominant role in the interaction with the polar residues of the CBR binding site.<sup>37</sup>

In the series of 8-unsubstituted derivatives 5a–d, 5v (Ro-15-1624), and 5x (Ro-23-2896) (Chart 3), the introduction of substituents in the 4'-position produces a slight affinity decrease when F, Cl, and CH<sub>3</sub> substituents are taken into consideration, while the effect is more marked in the case of 4'-methoxy derivative 5d. Differently, in the series of 8-chloro derivatives 5j–m, 5y (Ro-15-8670, Chart 3) the affinity decrease of about 1 order of magnitude is also observed in 4'-fluoro derivative 5j, 4'-chloro derivative 5k, and 4'-methyl derivative 5l. This discrepancy in the structure–affinity relationship trends suggests that the introduction of a chlorine atom in position 8 of the tricyclic nucleus leads to a charge redistribution in the benzofused ring, modulating the polar interaction within the binding site. A comparison of GABA ratio values suggests that the presence of a hydrogen atom in position 8 produces antagonist-like profiles. On the other hand, the imidazobenzodiazepine derivatives bearing a chlorine atom in the same position show different efficacy profiles spanning from the described<sup>60</sup> agonist properties of 5y to the antagonist ones shown by 4'-methyl derivative 5l and by

Scheme 7. Synthesis of Conformationally Constrained Derivative 7<sup>a</sup>

<sup>a</sup> Reagents: (i) LiAlH<sub>4</sub>, THF; (ii) TBDMSCl, imidazole, CH<sub>2</sub>Cl<sub>2</sub>; (iii) *t*-BuOK, ClPO(OEt)<sub>2</sub>, THF; (iv) CNCH<sub>2</sub>COOEt, *t*-BuOK; (v) *n*-Bu<sub>4</sub>NF, THF; (vi) NaH, DMF.

3'-nitro derivative **5n** through the partial agonist profiles of 4'-fluoro derivative **5j** and 4'-chloro derivative **5k**.

In order to obtain information on the bioactive conformation of these 6-phenylimidazo[1,5-*a*][1,4]benzodiazepine derivatives, the ester carbonyl of compound **5v** was constrained in *cis* position with respect to imidazole nitrogen as in lactone **7** (Figure 1). Unfortunately, compound **7** shows a CBR affinity in the submicromolar range very similar to that shown by 4-methyl derivative **5e** and about 1 order of magnitude lower than the unconstrained parent compound **5v**. Therefore, this conformational constraining approach is unsuitable for study of the interaction of these imidazodiazepine derivatives with CBR. The idea is that the introduction of a carbon atom in the 4-position of the tricyclic nucleus is not tolerated by the CBR binding site (compare **5v** with **5e** and **5f** with **5i**) and the alteration in the binding phenomenon (leading to submicromolar affinity) could mask the true effect of the carbonyl group constraining.

The modification of the ester side chain in 8,4'-dichloro derivative **5k** produced inactive compounds **5p–u**. Moreover, the benzo fusion of the pendent phenyl ring of **5y** leads to an affinity decrease of about 1 order of magnitude (compare **5o** with **5y**) and the same structural modification leading to compound **6** is not tolerated (compare **6** with **5b**).

**In Vitro Efficacy.** A second and more direct measure of *in vitro* efficacy was determined by a <sup>36</sup>Cl<sup>-</sup> uptake assay in rat cerebrocortical

synaptoneuroosomes.<sup>47,48</sup> The synaptic chloride conductance effected by GABA activating the GABA<sub>A</sub> receptor complex is modulated by ligands acting at the CBR. Full agonists increase current, and antagonists have no effect, while inverse agonists decrease ion flow. Among the title compounds, **5a,b,c,f,n** were selected and compared to flunitrazepam, flumazenil, and ethyl β-carboline, a full agonist, an antagonist, and an inverse agonist, respectively (Figure 2).

On the basis of the results obtained with these standards, it was possible to show the course of the uptake and to make a direct comparison with the compounds under examination. In particular, compounds **5a,b,n** did not show a significant modification of <sup>36</sup>Cl<sup>-</sup> influx, behaving in a manner similar to that of the antagonist flumazenil. Although a very slight decrease for compound **5b** and a modest increase for compound **5n** could be recognized, no effect on the ion flow seems to be elicited by compound **5a**. Thus, with some discrepancy with respect to their GABA ratio (GR) values [e.g., **5a** (GR = 0.77) and **5b** (GR = 0.84)], these compounds appear to behave as CBR antagonists as well as compound **5n**, the GABA ratio of which is very close to 1.0.

A quite different behavior is shown by compounds **5c,f**, the effect of which on <sup>36</sup>Cl<sup>-</sup> influx is surprising if their GABA ratio values, 0.97 and 1.0, respectively, are taken into account. In fact, the massive ion flow promoted by these compounds is completely unexpected, making the efficacy profile of **5c** similar to the one of a partial agonist, while that of **5f**, overlapping the flunitrazepam profile, is therefore typical of a full agonist. The rationalization of these results is far from obvious in light of the discrepancies observed when using the two different intrinsic efficacy determination methods.

**In Vivo Efficacy.** In order to assess the unexpected agonist properties, compound **5f** was examined in mice for its pharmacological effects. Four potential benzodiazepine actions were considered: potential anxiolytic effect was screened by means of light/dark box test, while the myorelaxant effect was measured by means of the rotarod test; the hole-board test was performed to verify the effect of **5f** on mouse spontaneous motility and explorative activity, and finally the mouse learning and memory impairment was evaluated by passive avoidance test.

Effects on mouse anxiety of the newly synthesized molecule and diazepam were studied by means of a light/dark box apparatus. In our experiments compound **5f** showed a statistically significant anxiolytic-like effect starting from a dose of 1.0 mg kg<sup>-1</sup> po, demonstrated by the increasing of time spent in the light compartment of the light/dark apparatus (Figure 3). At 10 mg/kg<sup>-1</sup> po, compound **5f** reached an effect comparable to that exhibited by the reference drug diazepam at 1.0 mg kg<sup>-1</sup> ip, showing the same efficacy but lower potency.

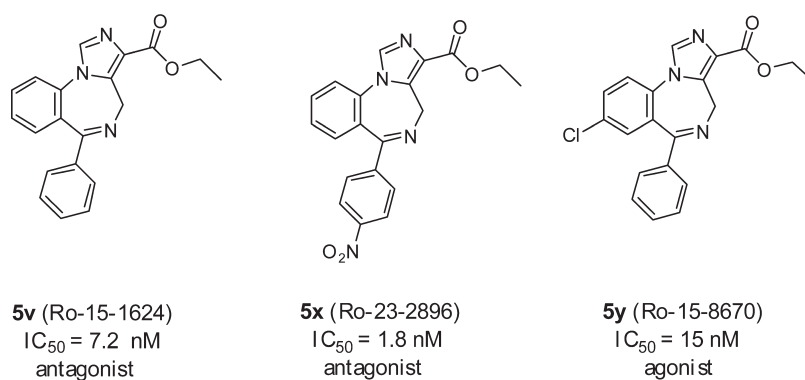
The effects of compound **5f** on animal motor coordination were investigated by means of the mouse rotarod test as a screening method to discover any myorelaxant effect (Figure 4). Compound **5f** at a dose of 10 mg kg<sup>-1</sup> po was unable to modify motor coordination, since **5f** did not increase the number of falls from the rotating rod. Diazepam at 1.0 mg kg<sup>-1</sup> ip showed a significant muscle relaxant effect (data not shown).

The hole board test, which is known to highlight neurological or muscular alterations, demonstrates that 10 mg kg<sup>-1</sup> po compound **5f** did not show significant differences either in spontaneous motility (number of movements) or in explorative activity (number of inspections) with respect to the carboxymethylcellulose (CMC) treated control mice (Figure 5).

**Table 1.** Inhibition of [ $^3\text{H}$ ]Flumazenil Specific Binding to Bovine and Human Cortical Membranes and GABA Ratios of the Title and Reference Compounds

compd	R	R <sub>1</sub>	R <sub>2</sub>	Ar	K <sub>i</sub> ± SEM <sup>d</sup> (nM)		GABA ratio <sup>b</sup>	
					bovine	human	bovine	human
5a	COOEt	H	H	<i>p</i> -fluorophenyl	11.5 ± 3.8	20.8 ± 0.2	0.77	0.96
5b (Ro-22-9735) <sup>c</sup>	COOEt	H	H	<i>p</i> -chlorophenyl	12.7 ± 1.1	22.5 ± 2.9	0.84	0.87
5c	COOEt	H	H	<i>p</i> -methylphenyl	11.4 ± 3.8	18.5 ± 2.5	0.97	1.10
5d	COOEt	H	H	<i>p</i> -methoxyphenyl	110 ± 25	120 ± 10.8	0.78	
5e	COOEt	H	Me	phenyl	453 ± 68.2	750 ± 65.8	1.30	
5f	COOEt	F	H	<i>p</i> -fluorophenyl	10.9 ± 2.5	22.3 ± 0.3	1.0	1.05
5g <sup>d</sup>	COOEt	F	H	<i>m</i> -nitrophenyl	4.4 ± 0.3	9.7 ± 0.7	1.19	1.20
5h <sup>d</sup>	COOEt	F	H	<i>p</i> -nitrophenyl	14.8 ± 1.4	20.0 ± 1.8	0.89	0.86
5i	COOEt	F	Me	<i>p</i> -fluorophenyl	510 ± 90.3	550 ± 50.7	1.19	
5j	COOEt	Cl	H	<i>p</i> -fluorophenyl	188 ± 35.2	212 ± 38.6	1.25	
5k	COOEt	Cl	H	<i>p</i> -chlorophenyl	236 ± 84.6	210 ± 23	1.30	
5l	COOEt	Cl	H	<i>p</i> -methylphenyl	199 ± 44.8	178 ± 38.3	1.05	
5m	COOEt	Cl	H	<i>p</i> -methoxyphenyl	210 ± 73.2	227 ± 45.4		
5n	COOEt	Cl	H	<i>m</i> -nitrophenyl	1.7 ± 0.2	2.3 ± 0.3	0.99	0.98
5o	COOEt	Cl	H	1-naphthyl	186 ± 78.2	216 ± 61.5	1.30	
5p	COO- <i>t</i> -Bu	Cl	H	<i>p</i> -chlorophenyl	1299 ± 280			
5q	CONH <sub>2</sub>	Cl	H	<i>p</i> -chlorophenyl	>10000			
5r	CONHMe	Cl	H	<i>p</i> -chlorophenyl	>10000			
5s	CONMe <sub>2</sub>	Cl	H	<i>p</i> -chlorophenyl	>10000			
5t	CN	Cl	H	<i>p</i> -chlorophenyl	1654 ± 220			
5u	5-(1 <i>H</i> -tetrazole)	Cl	H	<i>p</i> -chlorophenyl	>10000			
6					>10000			
7					283 ± 118		0.95	
flunitrazepam					5.17 ± 0.2	6.5 ± 0.5	1.68	1.60
flumazenil					1.9 ± 0.09	2.1 ± 0.08	1.03	1.01

<sup>a</sup> K<sub>i</sub> values are the mean ± SEM of three independent determinations. <sup>b</sup> GABA ratio = (K<sub>i</sub> without GABA)/(K<sub>i</sub> with 50 μM GABA). <sup>c</sup> See ref 40. <sup>d</sup> Compounds 5g,h are referred to in the introduction as 4a,b, respectively (see ref 37).

**Chart 3.** Structures, Affinity Values for CBR, and Intrinsic Activity of Compounds 5v–y<sup>46</sup>

In order to investigate the effect of compound 5f on learning and memory, the mice performance on “passive avoidance test”, an experiment in which the animal learns to avoid a noxious event by suppressing a particular behavior, was investigated. In this assay, the difference between the retention latencies of 5f-treated mice and CMC-treated controls was not statistically significant at any tested dose (0.1, 1.0, 3.0, and 10 mg kg<sup>-1</sup> po, data not shown), showing no amnesic effect. Moreover, the effect of 5f as

anti-amnesic compound was evaluated as the capability to prevent the amnesic effect of 1.5 mg kg<sup>-1</sup> scopolamine ip. At 3 mg kg<sup>-1</sup> po, compound 5f could significantly increase the retention session latency and at 10 mg kg<sup>-1</sup> po completely prevented the amnesic effect of scopolamine (Figure 6).

**Interaction with GABA Receptor Subtypes.** On the basis of the above results dealing with binding affinity, intrinsic activity, and behavioral tests, we decided to verify and evaluate the binding

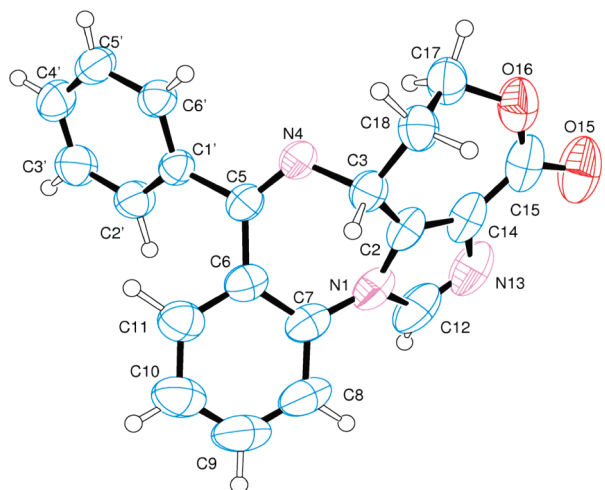


**Figure 1.** Crystal structure of compound 7. Ellipsoids enclose 50% probability.

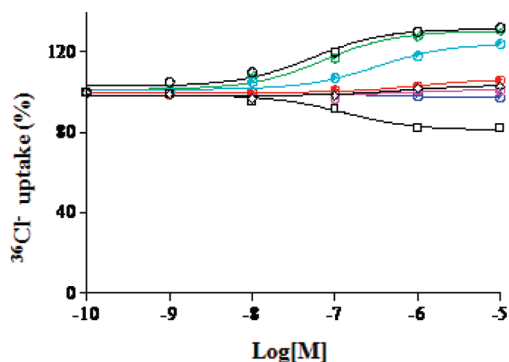


**Figure 2.**  $^{36}\text{Cl}^-$  uptake measured in rat cerebrocortical synaptosomes for compounds 5a (magenta), 5b (bleu), 5c (cyan), 5f (green), 5n (red), flunitrazepam (empty circles), flumazenil (empty diamonds), and ethyl  $\beta$ -carboline (empty squares).

### Anxiolytic Effect

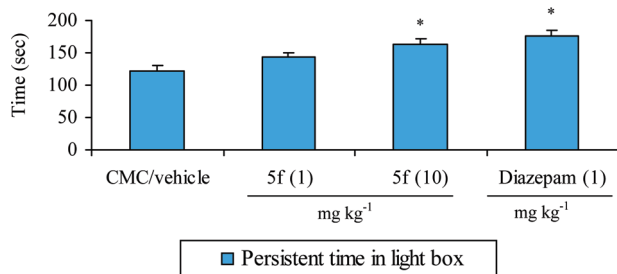


**Figure 3.** Anxiolytic effect. Each value represents the mean of at least 15–20 mice: ( $\wedge$ )  $P < 0.05$ , ( $*$ )  $P < 0.01$  vs saline/carboxymethylcellulose (CMC) treated mice.

properties and the pharmacologic profiles of the most representative imidazoesters **5b,c,f,g** toward the GABA receptor subtypes. In particular, isoforms of the  $\alpha$  subunit ( $\alpha_1$ ,  $\alpha_2$ , and  $\alpha_5$ ), which are the most implicated in the pharmacological effects

### Rota-rod Test

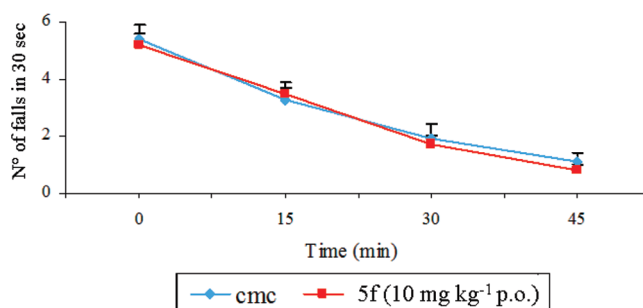


**Figure 4.** Effect on motor coordination 45 min after the treatment. Each value represents the mean of at least 15–20 mice: ( $\wedge$ )  $P < 0.05$ , ( $*$ )  $P < 0.01$  vs saline/CMC-treated mice.

### Hole Board Test

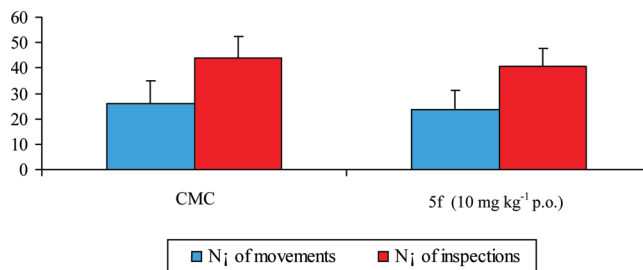


**Figure 5.** Effects on neurological or muscular alterations. Each value represents the mean of at least 15–20 mice: ( $\wedge$ )  $P < 0.05$ , ( $*$ )  $P < 0.01$  vs saline/CMC-treated mice.

### Passive Avoidance Test

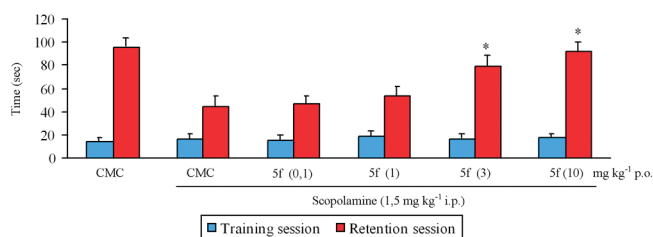


**Figure 6.** Learning and memory test. Each value represents the mean of at least 15–20 mice: ( $\wedge$ )  $P < 0.05$ , ( $*$ )  $P < 0.01$  vs saline/CMC-treated mice.

of CBR ligands, were evaluated by means of two different experimental approaches based on the two-electrode voltage clamp at GABA<sub>A</sub> receptor subtypes and radioligand assays, performed on HEK293 cells stably transfected with  $\alpha_2\beta_2\gamma_2$  or  $\alpha_5\beta_3\gamma_2$  isoform.

The two-electrode voltage-clamp technique was used as a first screening of compounds **5b,c,f,g** in order to assess their ability to modulate GABA-evoked  $\text{Cl}^-$  currents in *Xenopus laevis* oocytes expressing recombinant  $\alpha_1\beta_2\gamma_2\text{L}$ ,  $\alpha_2\beta_1\gamma_2\text{L}$ , and  $\alpha_5\beta_2\gamma_2\text{L}$  human GABA<sub>A</sub> receptors (Table 2). Compounds **5b,c,f,g** (1–10  $\mu\text{M}$ ) did not modify the responses of a GABA concentration equal to  $\text{EC}_{5-10}$  (approximately 3–6  $\mu\text{M}$  GABA) and did not show selectivity for a specific GABA subunit combination.

**Table 2. Modulation of GABA-Evoked Cl<sup>-</sup> Currents in *Xenopus laevis* Oocytes Expressing Recombinant  $\alpha_1\beta_2\gamma_2$ L,  $\alpha_2\beta_1\gamma_2$ L,  $\alpha_5\beta_2\gamma_2$ L Human GABA<sub>A</sub> Receptors Elicited by Compounds 5b,c,f,g at 1–10  $\mu$ M<sup>a</sup>**

$\mu$ M	$\alpha_1\beta_2\gamma_2$ L				$\alpha_2\beta_1\gamma_2$ L				$\alpha_5\beta_2\gamma_2$ L			
	5b	5c	5f	5g	5b	5c	5f	5g	5b	5c	5f	5g
0.01	+13 ± 7.3	ND	ND	ND	ND	ND	ND	ND	ND	ND	ND	ND
0.1	+1.0 ± 7.0	ND	ND	ND	ND	ND	ND	ND	ND	ND	ND	ND
1	+3.6 ± 4.1	+8.0 ± 39	-13 ± 9.2	+14 ± 15	-7.0 ± 7.4	0.0 ± 6.9	-7.5 ± 10	+10 ± 11	-0.5 ± 0.5	-4.0 ± 13	-1.0 ± 3.0	+27 ± 19
10	+6.3 ± 11	-4.0 ± 9.4	-12 ± 5.0	-24 ± 7.2	-18 ± 8.0	+8.3 ± 7.6	+6.5 ± 3.0	-3.3 ± 2.7	0.0 ± 5.0	-22 ± 6.5	-16 ± 5.5	-2.5 ± 9.5

<sup>a</sup> Each compound was preapplied for 60s before being coapplied for 30s with an EC<sub>5-10</sub> of GABA (3–6  $\mu$ M). Data, expressed as percent of control, are the mean ± SEM of two to three oocytes.

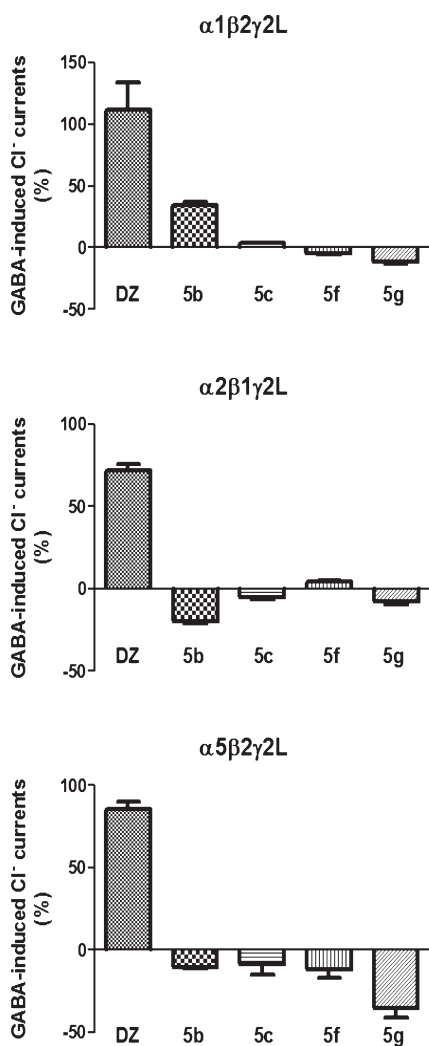


**Figure 7.** Effects of compounds 5b,c,f,g (10  $\mu$ M) on the diazepam (DZ) (1.0  $\mu$ M) enhancement of the GABA<sub>A</sub> receptor function in *Xenopus laevis* oocytes expressing (a)  $\alpha_1\beta_2\gamma_2$ L, (b)  $\alpha_2\beta_1\gamma_2$ L, and (c)  $\alpha_5\beta_2\gamma_2$ L human GABA<sub>A</sub> receptors. Data are expressed as percentage potentiation of the response induced by GABA at EC<sub>10</sub> and represent the mean ± SEM of two to three different oocytes.

Furthermore, in order to evaluate their pharmacological profile, the effects of the above-cited compounds (10  $\mu$ M) were tested on the diazepam (1.0  $\mu$ M) enhancement of the GABA<sub>A</sub> receptor function (Figure 7). In agreement with previous reports,<sup>49</sup> diazepam potentiated the action of an EC<sub>5-10</sub> concentration of

GABA in a reversible manner. However, the potentiation of the GABA response induced by diazepam was blocked when the oocytes were exposed to 5b,c,f,g (10  $\mu$ M). The ability of these compounds to block the effect of the benzodiazepine diazepam clearly demonstrates that these molecules act at the GABA<sub>A</sub> receptor via the benzodiazepine recognition site and that they are antagonists.

Subsequently, compounds 5c and 5f were studied in radioligand assays in HEK293 cells stably transfected with  $\alpha_2\beta_2\gamma_2$  or  $\alpha_5\beta_3\gamma_2$  GABA<sub>A</sub> receptor subtypes. The results showed that both compounds were able to bind to  $\alpha_2\beta_2\gamma_2$  receptor subtype with an affinity value in the nanomolar range (5c,  $K_i$  = 105 ± 10 nM; 5f,  $K_i$  = 60 ± 5 nM). In particular, the ability of compound 5f to bind to the  $\alpha_2$  subunit highlights the anxiolytic effects shown in the light/dark box test (Figure 3). In contrast, both compounds showed a significantly lower affinity toward  $\alpha_5\beta_3\gamma_2$  receptor subtype (5c,  $K_i$  = 908 ± 90 nM; 5f,  $K_i$  = 772 ± 70 nM). Anyway, 5f binding to the  $\alpha_5$  subunit could result in positive effects in learning and memory, as shown in the “passive avoidance test”.

**Molecular Modeling Studies.** In order to investigate at the molecular level the interactions that govern the recognition and binding of our ligands to the CBR, docking calculations by means of AutoDock 4.0 have been carried out using as target protein Cromer’s and the Ernst’s GABA<sub>A</sub> homology model.<sup>50</sup> In these calculations, only the interface between the  $\alpha$  and  $\gamma$  subunits, where the benzodiazepine binding site is known to be localized, has been considered as the docking area. Subsequently, the energy profile and the stability of the most interesting complexes as obtained from docking studies were assessed through extensive molecular dynamics (MD) studies and ab initio calculations.

Docking experiments, in the Cromer model, proposed similar binding conformations for compounds 5a–c,f,j, where the fused imidazole ring engages a  $\pi$ – $\pi$  interaction with Tyr210 and the fused benzene ring interacts with Phe100 and His102 residues (Figure 8A). Finally, the pendent phenyl moiety is involved in electron transfer interactions with Phe77 and Tyr58 rings. Even if the distance between the nitrogen at position 4 of the benzodiazepine ring and Thr142 is high for an H-bond formation (~4 Å), their proximity would suggest a possible interaction. All these favorable interactions contribute to achieve a good docking score (e.g., 5c AutoDock binding energy of –10.43 kcal/mol) and an inhibitory activity in the nanomolar range as it results from the experimental data.

Interestingly, the introduction of a bulkier side chain at position 3 such as the *tert*-butyl chain (5p) hampers the proper location of the ligand in the binding pocket, resulting in a decreased docking score (AutoDock binding energy of –6.53 kcal/mol). This is probably due to the steric clashes of the *tert*-butyl group

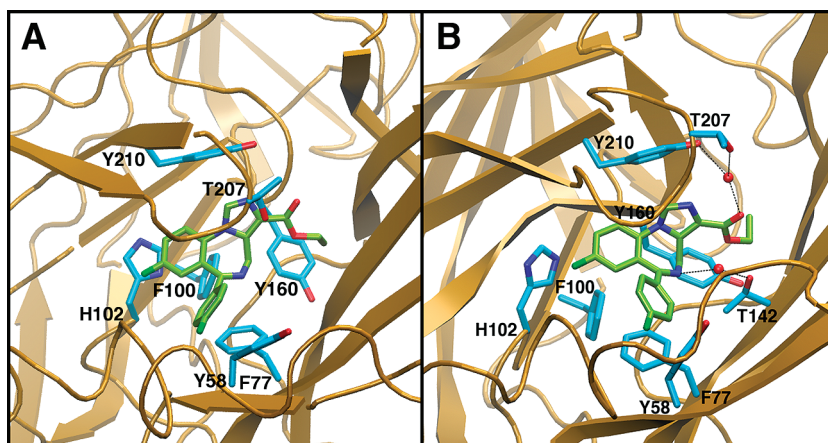


**Figure 8.** Binding conformation of **5f** in the CBR receptor as resulted from docking (A) and from subsequent MD (B). The ligand and the interacting residues are represented as green and cyan sticks, respectively, while the protein is represented as bronze cartoon. (B) The two interacting waters are shown as red spheres, while hydrogen atoms are not displayed for the sake of clarity.

with the backbone atoms of Tyr141 and Thr142, which are strongly held in place as they are part of a  $\beta$ -sheet. The decreased docking score of this compound is in line with its CBR reduced affinity, which is in the micromolar range, as measured in the binding assays. Since docking results obtained using Cromer's homology model might be affected by the approximation in the definition of the protein structure, we repeated the docking calculation of **5f** using Ernst's model. In the latter model, it was found that the benzodiazepine ring of **5f** is approximately located in the same region previously occupied in Cromer's model, but the pendent phenyl ring and the ester chain inverted their relative position. Thus, in Ernst's model, the ester chain fills the aromatic pocket formed by Phe77 and Tyr58 and the pendent phenyl ring fills the region formed by polar residues such as Thr141 and Thr207, where usually polar groups are bound. Moreover, while docking results in Cromer's model showed that only short ester chains are tolerated because of the presence of Tyr141 and Thr142 backbone, in Ernst's model this chain points outside the receptor and even bulkier ester groups might be allowed, in stark contrast with structure–activity relationship (SAR) data herein presented. The above-mentioned considerations prompted us to discard the docking results coming from Ernst's model. The major cause of the docking failure in this model was likely the orientation of the side chains of some residues such as ( $\alpha$ )-Arg144, ( $\alpha$ )-Tyr160, and ( $\gamma$ )-Asn128 that occupy the binding pocket, reducing the space available for the ligand binding. Thus, we decided to redo the docking calculations in the Ernst's model, optimizing these side chain positions to enlarge the region available for the ligand binding. Interestingly, when docking of **5f** is performed in such a model the best scored pose is highly similar to that found previously in Cromer's model. This supports the reliability of the binding mode proposed for **5f** and suggests that either model can be used for the study of the benzodiazepine binding once the binding pocket has been properly optimized.

Subsequently, with the aim to assess the energy profile and the stability of CBR (Cromer's model) in complex with compounds representative of the series such as **5a**, **f**, **j**, molecular dynamics (MD) studies were carried out. The three complexes showed different behaviors during MD simulations as detailed below. The complex between **5f** and CBR showed stable energetic and

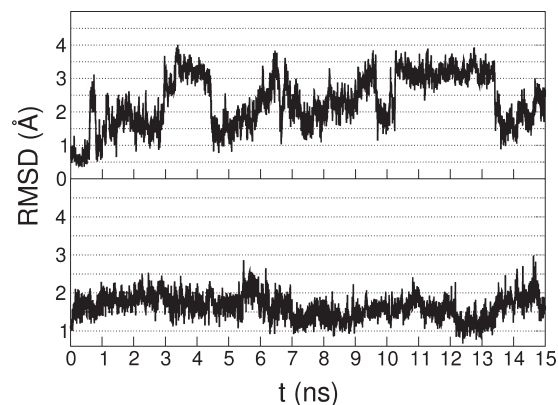


**Figure 9.** (Top) Plot of the rmsd of the heavy atoms of **5j** during MD simulation. The ligand changes its binding mode only after 1 ns of simulation. (Bottom) Plot of the rmsd of the heavy atoms of **5f** during MD simulation. This pose was very stable during the whole simulation.

geometric profiles, reinforcing the significance of our docking results and also addressing the relevant biological activity (see Table 1). In fact, the binding mode of **5f** does not substantially diverge from that calculated by the AutoDock program,<sup>51</sup> conserving all the main interactions with the protein (Figure 8). This is also clearly shown by the low root-mean-square deviation (rmsd) calculated on the heavy atoms of the ligand with respect to their coordinates at the beginning of the simulation (Figure 9).

In the found binding mode, the fused benzene ring of **5f** engages stable stacking interactions with Phe100 and His102 with the fluorine atom placed in a fruitful position to engage an halogen– $\pi$  interaction<sup>52</sup> with the imidazole ring of His102. The fused imidazole ring during the MD improves the geometry of its  $\pi$ – $\pi$  interaction with Tyr210 side chain, while the pendent phenyl moiety is involved in hydrophobic contacts with Phe77 and Tyr58 via a stacking and a T-shaped interaction, respectively. Moreover, during the whole simulation the carbonyl oxygen of the carboxy group is constantly involved in a H-bond interaction either directly with Thr207 or through a water bridge with Thr207 and Tyr210. Similarly, the nitrogen at position 4 of the benzodiazepine ring has been found to establish a H-bond with Thr142 either directly or via a neighboring water molecule.

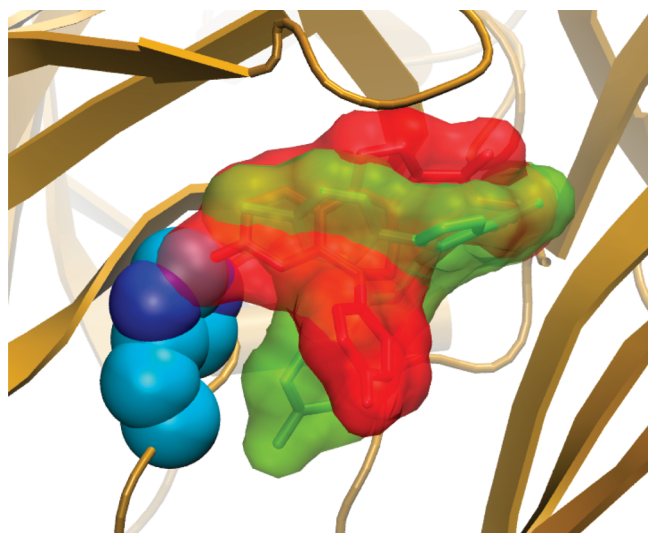


**Figure 10.** Representation of the binding conformation of **5j** in the CBR receptor at the beginning (red) and at the end (green) of the MD simulation. During the simulation, the ligand changes its conformation, either losing or weakening key interactions with the protein. The ligand is displayed as licorice under a transparent surface, while His102 is shown as space fill. The protein is represented as bronze cartoon, and hydrogen atoms are not displayed for the sake of clarity.

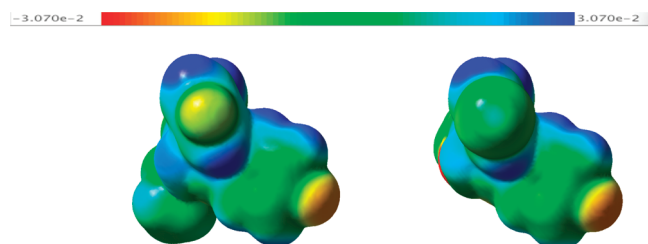


**Figure 11.** Electrostatic potential mapped onto the molecular surface of **5f** (left) and **5j** (right). The calculations were computed at the Hartree–Fock level of theory and using 6-31G\* as basis set. The scale of the electrostatic potential is  $-0.031$  (red) to  $0.031$  hartree (blue).

Notably, the described binding mode shares all the main interactions present in the refined benzodiazepine pharmacophore model.<sup>52b</sup> Particularly, the basic polar points, namely, H1 and H2 in the pharmacophore model, are here represented by the interactions with Thr207/Tyr210 and Thr142, respectively. The important lipophilic interaction L1 is that engaged with Ph100, while the additional lipophilic regions, namely, L2 and L3, are here formed by His102 and Tyr58/Phe77, respectively.

As for **5j**, MD simulation showed a weak stability of the binding conformation found by docking simulation (Figure 9). In fact, while AutoDock placed the ligand in a conformation very similar to that of **5f** in the CBR binding site, only after 1 ns of MD simulation, **5j** left the starting position adopting a different binding conformation with the fluorophenyl moiety pointing toward the inner part of the protein. The different behavior of **5f** and **5j** during the MD simulation, combined with the significantly lower CBR affinity shown by **5j** with respect to **5f**, prompted us to a more detailed investigation of the differences between the two ligands. Compound **5j** differs from **5f** for the presence of a chlorine atom in place of the fluorine in position 8 of the

imidazobenzodiazepine (IBDZ) nucleus of **5f**. The chlorine substituent is certainly bulkier than the fluorine one of **5f**, and the presence of a His102 side chain in the region of the binding site that hosts the halogen atom does not allow a comfortable allocation of the bulkier chlorine atom. Thus, the molecule slightly moves up in the binding site with the fused benzene ring located under the upper flexible loop and the fluorophenyl moiety pointing toward the inner part of the protein (Figure 10). Although most of the previously described ligand–protein interactions are conserved in this new binding conformation, some of them are either badly oriented or lost, like for instance the interaction between the fluorophenyl ring and the Tyr58 side chain.

In order to evaluate the differences in the electrostatic potential profile between **5f** and **5j**, ab initio calculations were performed to map the electrostatic potential of the two compounds onto the respective molecular surfaces representing the electron densities (Figure 11). While the fluorine atom of **5f** is entirely electronegative because of its small atomic radius, the bulkier chlorine atom of **5j** shows a considerably less negative charge. As a consequence, the halogen– $\pi$  interaction formed by **5f** with His102 side chain is stronger than that established by **5j**.

On the basis of our MD and ab initio calculations, we can conclude that the different electrostatic profiles of **5f** and **5j** together with the weaker interactions established by **5j** with CBR are at the base of the lower affinity of **5j** for CBR.

Our results on the binding modes of **5f** and **5j** are also useful to understand the behavior of compound **5a** within CBR. Here, although the halogen– $\pi$  interaction with His102 is no longer possible because of the presence of a hydrogen atom in place of the halogen at position 8 of the IBDZ nucleus, the small size of the hydrogen does not alter the placement of the ligand in the binding site. Consequently, similar to **5f**, the binding mode of **5a** during the MD simulation is stable conserving most of the above-described interactions with the surrounding residues and thus explaining the good affinity of this compound for CBR.

The coherence between docking and MD results supports the reliability of the proposed binding mode of **5f** to CBR.

## CONCLUSION

A series of 3-substituted 6-phenyl-4*H*-imidazo[1,5-*a*][1,4]-benzodiazepines and related compounds were designed and synthesized as central benzodiazepine receptor ligands. Among the newly synthesized compounds, 3-carboxyethyl esters showed high affinity for CBR with  $K_i$  values ranging from the low nanomolar to the submicromolar range and GABA ratio values spanning from 0.77 to 1.30. In particular, ethyl 8-fluoro-6-(4-fluorophenyl)-4*H*-imidazo[1,5-*a*][1,4]benzodiazepine-3-carboxylate (**5f**), in spite of its antagonist profile indicated by a GABA ratio value of 1.0, behaved as a full agonist in the classical animal model of anxiety light/dark box test and was devoid of the unpleasant side effects such as myorelaxation and amnesia. On the other hand, the CBR agonist profile of compound **5f** was confirmed when its efficacy was tested by means of  $^{36}\text{Cl}^-$  uptake and measured in rat cerebrocortical synaptosomes. In this test **5f** was capable of promoting a massive ion flux, mimicking the efficacy profile of a full agonist such as flunitrazepam.

Moreover, the selectivity of compounds **5b,c,f,g** has been assessed in recombinant  $\alpha_1\beta_2\gamma_2\text{L}$ ,  $\alpha_2\beta_1\gamma_2\text{L}$ , and  $\alpha_5\beta_2\gamma_2\text{L}$  human GABA<sub>A</sub> receptors, measuring their effects on the diazepam enhancement of the GABA<sub>A</sub> receptor function. These experiments

suggested that the selected compounds interacted with the benzodiazepine recognition site of GABA<sub>A</sub> receptor showing antagonist profiles. These results were confirmed when compounds **5c** and **5f** were studied in radioligand assays in HEK293 cells stably expressing  $\alpha_2\beta_2\gamma_2$  or  $\alpha_5\beta_3\gamma_2$  GABA<sub>A</sub> receptor subtype. The results showed that both compounds could bind to  $\alpha_2\beta_2\gamma_2$  receptor subtype with an affinity in the nanomolar range. In particular, the ability of compound **5f** to bind to the  $\alpha_2$  subunit supports the anxiolytic effects shown in the light/dark box test. In contrast, both compounds showed a significantly lower affinity toward  $\alpha_5\beta_3\gamma_2$  receptor subtype. Anyway, **5f** binding to the  $\alpha_5$  subunit could result in the positive effects in learning and memory, as shown in the “passive avoidance test”.

Finally, the most interesting compounds were studied in molecular docking simulations along with molecular dynamics experiments by using Cromer's GABA<sub>A</sub> homology model in order to better understand the ligand interactions at CBR. The docking experiments showed that only small substituents are well tolerated in the 4' position. Thus, compounds **5a–c,f** were able to interact profitably with key amino acids involved in the binding site, in agreement with the nanomolar range resulting from the experimental data, whereas the introduction of a bulkier lateral side chain (as in compound **5p**), with respect to the carboxyethyl one, prevents the correct binding mode from being established. The molecular dynamics calculation performed with the binary complexes formed by **5a**, **5f**, or **5j** with CBR demonstrated the stability of the binding mode and the main intermolecular interactions based on a large-time-scale simulation. The complex between **5f** and CBR showed stable energetic and geometric profiles, reinforcing the significance of our docking results and also addressing the relevant biological activity.

## EXPERIMENTAL SECTION

**Chemistry.** All chemicals used were of reagent grade. Yields refer to purified products and are not optimized. Melting points were determined in open capillaries on a Gallenkamp apparatus and are uncorrected. Merck silica gel 60 (230–400 mesh) was used for column chromatography. Merck TLC plates and silica gel 60 F<sub>254</sub> were used for TLC. <sup>1</sup>H NMR spectra were recorded with a Bruker AC 200 spectrometer in the indicated solvent (TMS as internal standard). The values of the chemical shifts are expressed in ppm, and the coupling constants (*J*) are expressed in Hz. Mass spectra were recorded on a VG 70-250S (EI, 70 eV), a Varian Saturn 3, or a ThermoFinnigan LCQdeca spectrometer.

The purity of compounds **5a–f,i–u**, **6**, and **7** was assessed by RP-HPLC and was found to be higher than 95%. A VWR Hitachi L-2130 pump system equipped with a VWR Hitachi L-2400 and with a Merck LiChroCART 125-4 C18 column was used in the HPLC analysis with (method A) acetonitrile–water–methanol (50:20:30) or (method B) methanol–acetonitrile (20:80) as the mobile phase at a flow rate of 0.7 mL/min. UV detection was achieved at 210 nm.

**General Procedure for the Synthesis of Compounds 5a–f, i–p.** A solution of the suitable 1,4-benzodiazepin-2-one **8a–f,i–o** (1.2 mmol) and potassium *tert*-butoxide (2.7 mmol) in dry THF (30 mL) was stirred at 0 °C for 10 min under argon and then treated with diethyl chlorophosphate (4.6 mmol). After the mixture was stirred for 30 min, the suitable isocyanacetate (6.1 mmol) was added. The resulting solution was stirred at 0 °C for 1 h and then allowed to stir at room temperature overnight. Acetic acid (1.8 mL) was added, and the mixture was stirred for an additional 20 min and then poured onto crushed ice to give a brownish solid. After filtration, the solid was dissolved in dichloromethane and the organic layer washed with brine,

dried over Na<sub>2</sub>SO<sub>4</sub>, filtered, and concentrated in vacuo. The residue was purified by flash chromatography with a suitable eluent to afford the expected imidazo ester, which after recrystallization from the suitable solvent gave an analytical sample.

**Ethyl 6-(4-Fluorophenyl)-4H-imidazo[1,5-a][1,4]benzodiazepine-3-carboxylate (5a).** The title compound was prepared starting from **8a** and following the above-cited general procedure (yield 29%). Colorless crystals were obtained from benzene–cyclohexane, mp 163–164 °C. HPLC (method A): retention time, 4.7 min; purity, 97.2%. <sup>1</sup>H NMR (CDCl<sub>3</sub>): 1.39 (t, 3H, *J* = 7.4), 4.02 (d, 1H, *J* = 12.5), 4.40 (m, 2H), 6.00 (d, 1H, *J* = 12.4), 7.02 (m, 2H), 7.43–7.55 (m, 4H), 7.59–7.71 (m, 2H), 7.91 (s, 1H). MS (ESI): *m/z* 350 (M + H<sup>+</sup>).

**Ethyl 6-(4-Chlorophenyl)-4H-imidazo[1,5-a][1,4]benzodiazepine-3-carboxylate (5b).** The title compound was resynthesized<sup>40</sup> starting from **8b** and following the above-cited procedure (yield 50%). Colorless crystals were obtained from cyclohexane–chloroform, mp 176–177 °C. HPLC (method A): retention time, 4.3 min; purity, 96.3%. <sup>1</sup>H NMR (CDCl<sub>3</sub>): 1.41 (t, 3H, *J* = 7.0), 4.07 (d, 1H, *J* = 12.1 Hz), 4.41 (m, 2H), 6.06 (d, 1H, *J* = 12.3 Hz), 7.30–7.73 (m, 8H), 7.92 (s, 1H). MS (ESI): *m/z* 366 (M + H<sup>+</sup>).

**Ethyl 6-(4-Methylphenyl)-4H-imidazo[1,5-a][1,4]benzodiazepine-3-carboxylate (5c).** The title compound was prepared starting from **8c** and following the above-cited procedure (yield 49%). Colorless crystals were obtained from diethyl ether, mp 141–142 °C. HPLC (method A): retention time, 4.1 min; purity, 98.4%. <sup>1</sup>H NMR (CDCl<sub>3</sub>): 1.41 (t, 3H, *J* = 7.0), 2.35 (s, 3H), 4.03 (d, 1H, *J* = 12.3 Hz), 4.41 (m, 2H), 6.03 (d, 1H, *J* = 12.6 Hz), 7.15–7.67 (m, 8H), 7.91 (s, 1H). MS (ESI): *m/z* 346 (M + H<sup>+</sup>).

**Ethyl 6-(4-Methoxyphenyl)-4H-imidazo[1,5-a][1,4]benzodiazepine-3-carboxylate (5d).** The title compound was prepared starting from **8d** and following the above-cited procedure to obtain a pale yellow oil (yield 45%). HPLC (method A): retention time, 3.7 min; purity, 98.2%. <sup>1</sup>H NMR (CDCl<sub>3</sub>): 1.44 (t, 3H, *J* = 7.0 Hz), 3.81 (s, 3H), 4.01 (d, 1H, *J* = 12.5 Hz), 4.37 (m, 2H), 5.98 (d, 1H, *J* = 12.4 Hz), 6.85 (d, 2H, *J* = 8.7 Hz), 7.42–7.52 (m, 5H), 7.58–7.65 (m, 1H), 7.87 (s, 1H). MS (ESI): *m/z* 362 (M + H<sup>+</sup>).

**Ethyl 4-Methyl-6-phenyl-4H-imidazo[1,5-a][1,4]benzodiazepine-3-carboxylate (5e).** The title compound was prepared starting from **8d** and following the above-cited procedure (yield 58%). Colorless crystals were obtained from cyclohexane, mp 168–169 °C. HPLC (method A): retention time, 5.3 min; purity, 97.2%. The <sup>1</sup>H NMR spectrum showed the existence of two diastereomeric conformations; for the sake of simplicity the integral intensities have not been given. <sup>1</sup>H NMR (CDCl<sub>3</sub>): 1.21 (d, *J* = 7.4), 1.39 (t, *J* = 7.6), 2.13 (d, *J* = 6.9), 4.26–4.44 (m), 6.63 (q, *J* = 7.2), 7.30–7.63 (m), 7.89 (s). MS (EI): *m/z* 345 (M<sup>+</sup>, 45).

**Ethyl 8-Fluoro-6-(4-fluorophenyl)-4H-imidazo[1,5-a][1,4]benzodiazepine-3-carboxylate (5f).** The title compound was prepared starting from **8f** and following the above-cited procedure (yield 28%). Yellow crystals were obtained from benzene–cyclohexane, mp 197–198 °C. HPLC (method A): retention time, 5.4 min; purity, 98.2%. <sup>1</sup>H NMR (CDCl<sub>3</sub>): 1.40 (t, 3H, *J* = 6.9), 4.03 (br d, 1H, *J* = 12.3), 4.35 (m, 2H), 6.03 (br d, 1H, *J* = 12.2), 7.00–7.15 (m, 3H), 7.32–7.42 (m, 1H), 7.47–7.60 (m, 3H), 7.87 (s, 1H). MS (EI): *m/z* 367 (M<sup>+</sup>, 49).

**Ethyl 8-Fluoro-6-(4-fluorophenyl)-4-methyl-4H-imidazo[1,5-a][1,4]benzodiazepine-3-carboxylate (5i).** The title compound was prepared starting from **8i** and following the above-cited procedure (yield 30%). Yellow crystals were obtained from benzene–cyclohexane, mp 245–246 °C. HPLC (method A): retention time, 6.5 min; purity, 97.5%. The <sup>1</sup>H NMR spectrum showed the existence of two diastereomeric conformations; for the sake of simplicity the integral intensities have not been given. <sup>1</sup>H NMR (CDCl<sub>3</sub>): 1.21 (d, *J* = 7.5), 1.39 (t, *J* = 7.4), 2.12 (d, *J* = 6.9), 4.23–4.44 (m), 6.64 (q, *J* = 7.2), 7.05 (m), 7.35 (m), 7.54 (m), 7.84 (s). MS (EI): *m/z* 381 (M<sup>+</sup>, 35).

**Ethyl 8-Chloro-6-(4-fluorophenyl)-4H-imidazo[1,5-a]-[1,4]benzodiazepine-3-carboxylate (5j).** The title compound was prepared starting from **8j** and following the above-cited procedure (yield 66%). Colorless crystals were obtained from benzene–cyclohexane, mp 203–204 °C. HPLC (method A): retention time, 5.3 min; purity, 96.2. <sup>1</sup>H NMR (CDCl<sub>3</sub>): 1.41 (t, 3H, *J* = 6.9), 4.03 (d, 1H, *J* = 12.4), 4.41 (m, 2H), 6.03 (d, 1H, *J* = 12.2), 7.01–7.65 (m, 7H), 7.89 (s, 1H). MS (EI): *m/z* 383 (M<sup>+</sup>, 64).

**Ethyl 8-Chloro-6-(4-chlorophenyl)-4H-imidazo[1,5-a]-[1,4]benzodiazepine-3-carboxylate (5k).** The title compound was prepared starting from **8k** and following the above-cited procedure (yield 58%). Colorless crystals were obtained from benzene–cyclohexane, mp 229–230 °C. HPLC (method A): retention time, 54 min; purity, 97.2%. <sup>1</sup>H NMR (CDCl<sub>3</sub>): 1.41 (t, 3H, *J* = 7.0), 4.03 (d, 1H, *J* = 12.0), 4.42 (m, 2H), 6.04 (d, 1H, *J* = 12.3), 7.34–7.56 (m, 6H), 7.65 (dd, 1H, *J* = 8.3, 2.1), 7.90 (s, 1H). MS (ESI): *m/z* 400 (M + H<sup>+</sup>).

**Ethyl 8-Chloro-6-(4-methylphenyl)-4H-imidazo[1,5-a]-[1,4]benzodiazepine-3-carboxylate (5l).** The title compound was prepared starting from **8l** and following the above-cited procedure (yield 30%). Colorless crystals were obtained from benzene, mp 232–233 °C. HPLC (method A): retention time, 4.4 min; purity, 97.5%. <sup>1</sup>H NMR (CDCl<sub>3</sub>): 1.39 (t, 3H, *J* = 7.2), 2.36 (s, 3H), 4.02 (d, 1H, *J* = 12.5), 4.39 (m, 2H), 6.02 (d, 1H, *J* = 12.4), 7.16 (d, 2H, *J* = 7.8), 7.36 (d, 2H, *J* = 7.9), 7.41 (d, 1H, *J* = 1.7), 7.49 (d, 1H, *J* = 8.5), 7.61 (dd, 1H, *J* = 8.8, 1.8), 7.87 (s, 1H). MS (EI): *m/z* 379 (M<sup>+</sup>, 49).

**Ethyl 8-Chloro-6-(4-methoxyphenyl)-4H-imidazo[1,5-a]-[1,4]benzodiazepine-3-carboxylate (5m).** The title compound was prepared starting from **8m** and following the above-cited procedure (yield 44%). Colorless crystals were obtained from diethyl ether, mp 180–181 °C. HPLC (method A): retention time, 3.6 min; purity, 99.2%. <sup>1</sup>H NMR (CDCl<sub>3</sub>): 1.40 (t, 3H, *J* = 7.0), 3.81 (s, 3H), 3.99 (d, 1H, *J* = 12.5), 4.40 (m, 2H), 5.98 (d, 1H, *J* = 12.5), 6.86 (d, 2H, *J* = 8.7), 7.41–7.52 (m, 4H), 7.61 (dd, 1H, *J* = 8.5, 2.2), 7.87 (s, 1H). MS (EI): *m/z* 395 (M<sup>+</sup>, 54).

**Ethyl 8-Chloro-6-(3-nitrophenyl)-4H-imidazo[1,5-a]-[1,4]benzodiazepine-3-carboxylate (5n).** The title compound was prepared starting from **8n** and following the above-cited procedure (yield 66%). Colorless crystals were obtained from benzene–cyclohexane, mp 258–260 °C. HPLC (method A): retention time, 3.7 min; purity, 96.1%. <sup>1</sup>H NMR (CDCl<sub>3</sub>): 1.41 (t, 3H, *J* = 7.0), 4.10 (d, 1H, *J* = 12.7), 4.42 (m, 2H), 6.12 (d, 1H, *J* = 12.8), 7.35 (d, 1H, *J* = 2.0), 7.55–7.73 (m, 3H), 7.87–7.93 (m, 2H), 8.27–8.37 (m, 2H). MS (EI): *m/z* 410 (M<sup>+</sup>, 70).

**Ethyl 8-Chloro-6-(1-naphthyl)-4H-imidazo[1,5-a]-[1,4]benzodiazepine-3-carboxylate (5o).** The title compound was prepared starting from **8o** and following the above-cited procedure (yield 38%). Colorless crystals were obtained from benzene–cyclohexane, mp 193–194 °C. HPLC (method A): retention time, 3.9 min; purity, 97.2%. <sup>1</sup>H NMR (CDCl<sub>3</sub>): 1.39 (t, 3H, *J* = 7.1), 4.20 (br s, 1H), 4.39 (q, 2H, *J* = 7.2), 6.10 (br s, 1H), 7.18 (s, 1H), 7.32–7.56 (m, 7H), 7.83–7.92 (t, 2H, *J* = 8.8), 8.00 (s, 1H). MS (EI): *m/z* 415 (M<sup>+</sup>, 80).

**tert-Butyl 8-Chloro-6-(4-chlorophenyl)-4H-imidazo[1,5-a]-[1,4]benzodiazepine-3-carboxylate (5p).** The title compound was prepared starting from **8k** and following the above-cited procedure (yield 30%). Colorless crystals were obtained from benzene–cyclohexane, mp 230–231 °C. HPLC (method A): retention time, 6.6 min; purity, 99.6%. <sup>1</sup>H NMR (CDCl<sub>3</sub>): 1.61 (s, 9H), 4.00 (d, 1H, *J* = 12.5), 6.02 (d, 1H, *J* = 12.8 Hz), 7.32–7.52 (m, 6H), 7.62 (dd, 1H, *J* = 8.5, 2.1), 7.86 (s, 1H).

**Ethyl 6-(4-Chlorophenyl)-4H-imidazo[1,5-a]naphtho[2,1-f]-[1,4]diazepine-3-carboxylate (6).** The title compound was prepared starting from **10** and following the above-cited procedure (yield 48%). Colorless crystals were obtained from ethanol–ethyl acetate, mp 277–278 °C. HPLC (method A): retention time, 5.2 min; purity, 99.0%. <sup>1</sup>H NMR (CDCl<sub>3</sub>): 1.44 (t, 3H, *J* = 7.1), 4.08 (d, 1H, *J* = 12.5),

4.44 (m, 2H), 6.05 (d, 1H, *J* = 12.3), 7.37 (m, 3H), 7.52 (m, 2H), 7.71 (m, 2H), 7.90 (d, 1H, *J* = 8.6), 8.01 (m, 1H), 8.10 (s, 1H), 8.14 (m, 1H). MS (EI): *m/z* 415 (M<sup>+</sup>, 10).

**General Procedure for the Synthesis of Diazepinone Derivatives 8a–d,f,j–o and 10.** The synthesis of diazepinone derivatives **8a–d,f,j–o** and **10** was carried out starting from the suitable 2-aminobenzophenones following well-known procedures.<sup>37,39,40</sup>

**General Procedure for the Synthesis of Carboxamides 5q–s.** A solution of acid **16** (0.49 mmol) in CHCl<sub>3</sub> (3.0 mL) and TEA (0.070 mL, 0.95 mmol) was cooled at 15 °C and treated with isobutyl chloroformate (0.51 mmol) while stirring at 15 °C for 1 h. The reaction mixture was treated with a suitable amine (0.50 mmol) (for **5q**, gaseous NH<sub>3</sub> was bubbled into the reaction mixture until an insoluble residue appeared), stirred at the same temperature for 30 min, poured into ice–water, and then extracted with CH<sub>2</sub>Cl<sub>2</sub>. The organic layer was washed with brine, dried over Na<sub>2</sub>SO<sub>4</sub>, and evaporated under reduced pressure. The resulting solid was recrystallized from a suitable solvent to afford an analytical sample of the expected compound.

**8-Chloro-6-(4-chlorophenyl)-4H-imidazo[1,5-a]-[1,4]benzodiazepine-3-carboxamide (5q).** The title compound was prepared following the above-cited procedure (yield 83%). White crystals were obtained from benzene–cyclohexane, mp >300 °C. HPLC (method A): retention time, 2.6 min; purity, 97.6%. <sup>1</sup>H NMR (CDCl<sub>3</sub>): 4.03 (d, 1H, *J* = 13.3), 5.32 (br s, 1H), 6.21 (d, 1H, *J* = 13.8 Hz), 6.93 (br s, 1H), 7.31–7.39 (m, 3H), 7.43–7.52 (m, 3H), 7.62 (dd, 1H, *J* = 8.9, 2.6), 7.80 (s, 1H).

**8-Chloro-6-(4-chlorophenyl)-N-methyl-4H-imidazo[1,5-a]-[1,4]benzodiazepine-3-carboxamide (5r).** The title compound was prepared following the above-cited procedure (yield 60%). Colorless crystals were obtained from benzene–cyclohexane, mp 267–268 °C. HPLC (method A): retention time, 3.4 min; purity, 98.8%. <sup>1</sup>H NMR (CDCl<sub>3</sub>): 2.95 (d, 3H, *J* = 4.9), 4.03 (d, 1H, *J* = 11.9), 6.24 (d, 1H, *J* = 12.0), 7.07 (br s, 1H), 7.30–7.55 (m, 6H), 7.62 (dd, 1H, *J* = 8.6, 2.6), 7.77 (s, 1H).

**8-Chloro-6-(4-chlorophenyl)-N,N-dimethyl-4H-imidazo[1,5-a]-[1,4]benzodiazepine-3-carboxamide (5s).** The title compound was prepared following the above-cited procedure (yield 79%). Colorless crystals were obtained from benzene–cyclohexane, mp 252–253 °C. HPLC (method A): retention time, 3.8 min; purity, 99.8%. <sup>1</sup>H NMR (CDCl<sub>3</sub>): 3.07 (s, 3H), 3.31 (s, 3H), 4.05 (d, 1H, *J* = 12.8), 5.85 (d, 1H, *J* = 12.8), 7.32–7.37 (m, 3H), 7.42–7.52 (m, 3H), 7.62 (dd, 1H, *J* = 8.7, 2.8), 7.82 (s, 1H).

**8-Chloro-6-(4-chlorophenyl)-3-(1H-tetrazol-5-yl)-4H-imidazo[1,5-a]-[1,4]benzodiazepine (5u).** A mixture of **5t** (0.27 mmol) in dry xylene (4.0 mL) containing 0.53 mmol of trimethyltin azide was heated at 115 °C for 41 h under argon. The precipitate was collected by filtration, washed with hot toluene, and dried under reduced pressure. A mixture of the solid in CH<sub>2</sub>Cl<sub>2</sub> (5.0 mL) and THF (1.0 mL) was treated with 10 N NaOH (0.02 mL, 0.2 mmol) and stirred at room temperature for 1 h. Triphenylmethyl chloride (0.114 mmol) was then added, and the reaction mixture was stirred at the same temperature for 3 h, then poured into ice–water and extracted with CH<sub>2</sub>Cl<sub>2</sub>. The organic layer was washed with brine, dried over Na<sub>2</sub>SO<sub>4</sub>, and concentrated under reduced pressure. The resulting residue was dissolved in THF (4.0 mL) and 10% HCl (2.0 mL), and the resulting mixture was stirred at room temperature for 4 h, then neutralized with 10% NaOH. The solvent was evaporated under reduced pressure to afford a solid, which was recrystallized from benzene–cyclohexane to give the analytical sample of **5u** as colorless crystals (mp >300 °C, yield 37%). HPLC (method B): retention time, 6.6 min; purity, 96.2%. <sup>1</sup>H NMR (DMSO-*d*<sub>6</sub>): 4.30 (d, 1H, *J* = 12.0), 5.87 (d, 1H, *J* = 12.0), 7.43 (m, 1H), 7.47 (m, 4H), 7.85–7.99 (m, 2H), 8.55 (s, 1H). MS (ESI): *m/z* 395 (M – H<sup>+</sup>).

**8-Chloro-6-(4-chlorophenyl)-4H-imidazo[1,5-a]-[1,4]benzodiazepine-3-carbonitrile (5t).** A mixture of compound **5q** (0.4 mmol) in dry benzene (7.0 mL) was treated while stirring with

POCl<sub>3</sub> (4 mmol) and refluxed for 7 h. The mixture was then treated with of CH<sub>2</sub>Cl<sub>2</sub> (2.0 mL), a saturated solution of NaHCO<sub>3</sub> (2.0 mL) and stirred at room temperature for 12 h. The organic layer was separated and washed until neutral, dried over Na<sub>2</sub>SO<sub>4</sub>, and evaporated under reduced pressure to give a solid, which was recrystallized from benzene–cyclohexane to afford **5t** colorless crystals (mp 249–250 °C, yield 47%). HPLC (method A): retention time, 3.8 min; purity, 98.4%. <sup>1</sup>H NMR (CDCl<sub>3</sub>): 4.12 (d, 1H, *J* = 11.8), 5.39 (d, 1H, *J* = 11.9), 7.33–7.46 (m, 5H), 7.53 (d, 1H, *J* = 8.7) 7.66 (dd, 1H, *J* = 8.2, 2.0), 7.90 (s, 1H). MS (EI): *m/z* 352 (M<sup>+</sup>, 100).

**Lactone 7.** A solution of compound **20** (0.14 mmol) in dry DMF (7.0 mL) was cooled at 0 °C, treated with NaH (0.20 mmol), and kept at this temperature for 30 min. The ice bath was removed, and the reaction mixture was stirred at 120 °C for 5 h, poured into ice–water, and then extracted with CH<sub>2</sub>Cl<sub>2</sub>. The organic layer was washed with water and brine, then dried over Na<sub>2</sub>SO<sub>4</sub>, and concentrated in vacuo. The resulting brown oil, when treated with a mixture of diethyl ether–*n*-hexane, gave a yellowish solid which after recrystallization from ethyl acetate afforded compound **7** as yellow crystals (yield 43%, mp 258–259 °C). HPLC (method A): retention time, 3.4 min; purity, 98.4%. <sup>1</sup>H NMR (CDCl<sub>3</sub>): 2.58 (m, 1H), 2.78 (m, 1H), 4.40 (m, 1H), 4.59 (dd, 1H, *J* = 13.0, 6.4), 4.93 (dd, 1H, *J* = 12.9, 8.6), 7.31–7.51 (m, 7H), 7.59–7.74 (m, 2H), 8.04 (s, 1H). MS (EI): *m/z* 329 (M<sup>+</sup>, 100).

**X-ray Crystallography.** A single crystal of **7** was submitted to X-ray data collection by means of a Siemens P4 four-circle diffractometer at 293 K equipped with a graphite monochromated Mo K $\alpha$  radiation ( $\lambda$  = 0.710 69 Å). The structure was solved by direct methods implemented in the SHELXS-97 program.<sup>53</sup> The refinements were carried out by full-matrix anisotropic least-squares on *F*<sup>2</sup> for all reflections for non-H atoms by means of the SHELXL-97 program.<sup>54</sup>

Crystallographic data (excluding structure factors) of this crystal structure have been deposited with the Cambridge Crystallographic Data Centre as supplementary publication number CCDC 805673. Copies of the data can be obtained, free of charge, on application to CCDC, 12 Union Road, Cambridge CB2 1EZ, U.K. [fax, 144-(0)1223-336033; e-mail, deposit@ccdc.cam.ac.uk].

**Radioligand Binding Studies in Native Bovine and Human Cerebral Receptors.** [<sup>3</sup>H]Flumazenil (specific activity of 70.8 Ci/mmol) was obtained from Perkin-Elmer Life Science (Milano, Italy). All other chemicals were at reagent grade and were obtained from commercial suppliers.

Bovine cortex was obtained from the local slaughterhouse. Human cortex samples were taken post-mortem at the Department of Pathological Anatomy, University of Pisa, Italy, during autopsy sessions. The subjects had died from causes not primarily involving the brain and had not suffered from any psychiatric or neurological disorders. The time between death and tissue dissection/freezing ranged from 18 to 36 h. The samples were immediately packed in dry ice and stored in a –80 °C freezer. The study was approved by the Ethics Committee of the University of Pisa, Italy.

Bovine and human cerebral cortex membranes were prepared in accordance with Martini et al.<sup>55</sup> Briefly, cerebral cortex was homogenized in 10 volumes of ice cold 0.32 M sucrose containing protease inhibitors. The homogenate was centrifuged at 1000g for 10 min at 4 °C. The resulting pellet was discarded, and the supernatant was recentrifuged at 48000g for 15 min at 4 °C. Then the pellet was osmotically shocked by suspension in 10 volumes of 50 mM Tris-citrate buffer at pH 7.4 containing protease inhibitors and recentrifuged at 48000g for 15 min at 4 °C. The resulting membranes were frozen and washed by means of a procedure previously described for removing endogenous GABA from cerebral cortex.<sup>56</sup> Finally, the pellet was suspended in 10 volumes of 50 mM Tris-citrate buffer, pH 7.4, and used in the binding assay. Protein concentration was assayed by the method of Lowry et al.<sup>57</sup> by means of bovine serum albumin as the standard.

[<sup>3</sup>H]Flumazenil binding studies were performed as previously reported.<sup>58</sup> The [<sup>3</sup>H]flumazenil binding was performed in triplicate by incubating aliquots of the membrane fractions (0.2–0.3 mg of protein) at 0 °C for 90 min in 0.5 mL of 50 mM Tris-citrate buffer, pH 7.4, with approximately 0.2 nM [<sup>3</sup>H]flumazenil. Nonspecific binding was defined in the presence of 10  $\mu$ M diazepam. After incubation, the samples were diluted at 0 °C with 5 mL of the assay buffer and immediately harvested onto GF/B filters (Brandel) by means of a harvester and washed with ice-cold assay buffer. The filters were washed twice with 5 mL of the buffer, dried, and an amount of 4 mL of Ready Protein Beckman scintillation cocktail was added; radioactivity was counted in a Packard LS 1600 liquid-phase scintillation  $\beta$  counter.

Compounds were routinely dissolved in DMSO and added to the assay mixture to a final volume of 0.5 mL. Blank experiments were carried out to determine the effect of the solvent (2%) on binding. At least six different concentrations spanning 3 orders of magnitude, adjusted approximately for the IC<sub>50</sub> of each compound, were used. IC<sub>50</sub> values, computer-generated by a nonlinear formula on a computer program (GraphPad, San Diego, CA), were converted to *K*<sub>i</sub> values, the *K*<sub>d</sub> values of radioligand in these different tissues calculated by the Cheng and Prusoff equation being known.<sup>59</sup> The *K*<sub>d</sub> of [<sup>3</sup>H]flumazenil binding to cortex membrane from bovine and human was 0.85 and 0.91 nM, respectively. The GABA ratio was determined by calculating (*K*<sub>i</sub> without GABA)/(*K*<sub>i</sub> with 50  $\mu$ M GABA) for each compound.

**Functional Efficacy Studies (<sup>36</sup>Cl<sup>–</sup> Uptake Studies).** <sup>36</sup>Cl<sup>–</sup> (specific activity 9.69  $\mu$ Ci/g) was obtained from Perkin-Elmer Life Science (Milan, Italy). All other chemicals were reagent grade and were obtained from commercial suppliers.

<sup>36</sup>Cl<sup>–</sup> uptake was measured in rat cerebrocortical synaptoneuro-somes as described by Schwartz et al.,<sup>47</sup> with minor modifications. Briefly, cerebral cortex was dissected from Sprague–Dawley male rats suspended 1:10 with ice-cold solution containing 145 mM NaCl, 5 mM KCl, 5 mM MgCl<sub>2</sub>, 1 mM CaCl<sub>2</sub>, 10 mM HEPES, pH 7 (T1 buffer), and 10 mM D-glucose; they were homogenized with a glass–glass homogenizer (five strokes) and filtered through three layers of nylon mesh (160  $\mu$ m) and a 10  $\mu$ m Millipore filter. The filtrates were centrifuged at 1000g for 15 min. After the supernatant was discarded, the pellet was gently resuspended in T1 buffer and washed once more by centrifugation (1000g for 15 min). The final pellet containing the synaptoneuro-somes was suspended 1:2 in T1 buffer and was kept on ice until ready for assay (no longer than 30 min).

Aliquots of synaptoneurosome suspensions (1.5–2 mg of protein) were preincubated at 30 °C for 10 min prior to the addition of 0.2  $\mu$ Ci <sup>36</sup>Cl<sup>–</sup>. Drugs were added simultaneously with the <sup>36</sup>Cl<sup>–</sup> (0.35 mL total assay volume). <sup>36</sup>Cl<sup>–</sup> uptake was stopped 10 s later by the addition of 5 mL of ice-cold HEPES, followed by vacuum filtration through glass fiber filters (Whatman GF/B) that had been soaked with 0.05% polyethylenimine to reduce nonspecific binding of <sup>36</sup>Cl<sup>–</sup>. The filters were washed three more times with 5 mL of ice-cold buffer and placed into scintillation vials containing 4 mL of Ready Protein Beckman scintillation cocktail, and radioactivity was counted in a Packard LS 1600 liquid-phase scintillation  $\beta$  counter. Data are expressed as percent stimulation of <sup>36</sup>Cl<sup>–</sup> uptake above basal level.

**Pharmacological Methods.** The experiments were carried out in accordance with the Animal Protection Law of the Republic of Italy, DL No. 116/1992, based on the European Communities Council Directive of November 24, 1986 (86/609/EEC). All efforts were made to minimize animal suffering and to reduce the number of animals involved. Male CD-1 albino mice (22–24 g) and male Swiss Webster (20–26 g) (Morini, Italy) were used. Twelve mice were housed per cage and fed a standard laboratory diet, with tap water ad libitum for 12 h/12 h light/dark cycles (lights on at 7:00). The cages were brought into the experimental room the day before the experiment for acclimatization purposes. All experiments were performed between 10:00 and 15:00.

**Rotarod Test.** The integrity of the animals' motor coordination was assessed using a rotarod apparatus (Ugo Basile, Varese, Italy) at a rotating speed of 16 rpm. The treatment was performed before the test. The numbers of falls from the rod were counted for 30 s, 30 min after drug administration, and the test was performed according to the method described by Vaught et al.<sup>60</sup>

**Light/Dark Box Test.** The apparatus (50 cm long, 20 cm wide, and 20 cm high) consisted of two equal acrylic compartments, one dark and one light, illuminated by a 60 W bulb lamp and separated by a divider with a 10 cm × 3 cm opening at floor level. Each mouse was tested by placing it in the center of the lighted area, away from the dark one, and allowing it to explore the novel environment for 5 min. The number of transfers from one compartment to the other and the time spent in the illuminated side were measured. This test exploited the conflict between the animal's tendency to explore a new environment and its fear of bright light.<sup>61</sup>

**Passive-Avoidance Test.** The test was performed according to the step-through method described by Jarvik et al.<sup>62</sup> The apparatus consisted of a two-compartment acrylic box with a lighted compartment connected to a darkened one by a guillotine door. As soon as the mouse entered the dark compartment, it received a thermal shock punishment. The latency times for entering the dark compartment were measured in the training test and after 24 h in the retention test. The maximum entry latency allowed in the training and retention sessions was, respectively, 60 and 180 s.

**Hole Board Test.** The hole board test consisted of a 40 cm<sup>2</sup> plane with 16 flush-mounted cylindrical holes (3 cm diameter) distributed 4 × 4 in an equidistant, grid-like manner. Mice were placed on the center of the board one by one and allowed to move about freely for a period of 5 min each. Two electric eyes, crossing the plane from midpoint to midpoint of opposite sides, thus dividing the plane into four equal quadrants, automatically signaled the movement of the animal (counts in 5 min) on the surface of the plane (spontaneous motility). Miniature photoelectric cells in each of the 16 holes recorded (counts in 5 min) the exploration of the holes (exploratory activity) by the mice. A total of 12–15 mice per group were tested.<sup>63</sup>

**Drugs.** Diazepam (Valium 10, Roche) and pentylentetrazole (PTZ, Sigma) were used. All drugs were dissolved in isotonic (NaCl 0.9%) saline solution and injected sc/ip. The new compound was administered by the po route and was suspended in 1% carboxymethylcellulose sodium salt and sonicated immediately before use. Drug concentrations were prepared in such a way that the necessary dose could be administered in a 10 mL/kg volume of carboxymethylcellulose (CMC) 1% by the po, ip, or sc route.

**Statistical Analysis.** All experimental results are given as the mean ± SEM. Each value represents the mean of 25 mice. An analysis of variance, ANOVA, followed by Fisher's protected least significant difference procedure for post hoc comparison, was used to verify significance between two mean values of behavioral results. The data were analyzed with the StatView software for Macintosh (1992). *P* values of less than 0.05 were considered significant.

**Radioligand Binding Studies in Recombinant  $\alpha_1\beta_2\gamma_2L$ ,  $\alpha_2\beta_1\gamma_2L$ , and  $\alpha_5\beta_2\gamma_2L$  Human GABA<sub>A</sub> Receptors Expressed in *Xenopus laevis* Oocytes and in HEK293 Cells.** For *Xenopus laevis* oocyte experiments, the cDNAs encoding human  $\alpha_1$ ,  $\alpha_2$ ,  $\alpha_5$ ,  $\beta_1$ ,  $\beta_2$ , or  $\gamma_2L$  GABA receptor subunits subcloned in pCDM8 vector were used for nuclear injections. Isolation of *Xenopus laevis* oocytes, cDNA injections, and two-electrode voltage-clamp recordings at a holding potential of −70 mV were performed as previously described.<sup>64</sup> The  $\alpha_1\beta_2\gamma_2L$ ,  $\alpha_2\beta_1\gamma_2L$ ,  $\alpha_5\beta_2\gamma_2L$  receptor subunit combinations were injected into the animal poles of the oocytes according to the blind method described by Colman<sup>65</sup> in a 1:1 ratio (1.5 ng/30 nL). Measurements were performed in oocytes 1–4 days after injection. Oocytes expressing  $\alpha_1\beta_2\gamma_2L$ ,  $\alpha_2\beta_1\gamma_2L$ ,  $\alpha_5\beta_2\gamma_2L$  receptors were placed in a chamber (approximately 100  $\mu$ L volume) and perfused (2 mL/min)

with modified Barth solution (MBS) containing (in mM) 88 NaCl, 1 KCl, 2.4 NaHCO<sub>3</sub>, 10 HEPES, 0.82 MgSO<sub>4</sub>, 0.33 Ca(NO<sub>3</sub>)<sub>2</sub>, 0.91 CaCl<sub>2</sub>. GABA was dissolved in MBS and applied for 30s. Diazepam, **5b**, **5c**, **5f**, or **5g** was first dissolved in dimethylsulfoxide (DMSO) and then diluted in MBS. The final DMSO concentration in MBS was 0.1%. This concentration did not affect the GABA responses. Experiments were performed by using a concentration of GABA corresponding to the EC<sub>5–10</sub> (i.e., a concentration that produced peak currents equal to 5–10% of a maximal GABA concentration). Drugs were preapplied for 60s before being coapplied with GABA for 30 s.

Radioligand binding studies at GABA<sub>A</sub> receptor subtypes expressed in HEK293 cells were assessed as previously described.<sup>63,66</sup> Clonal mammalian cell lines, expressing relatively high levels of GABA<sub>A</sub> receptor subtypes ( $\alpha_2\beta_2\gamma_2$ ,  $\alpha_5\beta_3\gamma_2$ ), were maintained in Eagle's minimum essential medium with EBSS, supplemented with 10% fetal calf serum, L-glutamine (2 mM), penicillin (100 U/mL), and streptomycin (100  $\mu$ g/mL) in a humidified atmosphere of 5% CO<sub>2</sub>, 95% air at 37 °C.

After removal, the cells were harvested by centrifugation at 500g. The crude membranes were prepared after homogenization in 10 mM potassium phosphate, pH 7.4, and differential centrifugation at 48000g for 30 min at 4 °C. The pellets were washed twice in this manner before final resuspension in 10 mM potassium phosphate, pH 7.4, that contained 100 mM potassium chloride and [<sup>3</sup>H]flumazenil. Binding assays to transfected cell membranes were carried out as previously described. Briefly, the cell line membranes were incubated in a volume of 500  $\mu$ L, which contained [<sup>3</sup>H]flumazenil at 1–2 nM and the test compound in the 10<sup>−9</sup>–10<sup>−5</sup> M range. Nonspecific binding was defined by 10<sup>−5</sup> M diazepam. Assays were incubated to equilibrium for 1 h at 4 °C. The compounds were dissolved in DMSO, the level of which did not exceed 1% and which was kept constant in all tubes. At least six different concentrations of each compound were used. The data of *n* = 3 experiments carried out in triplicate were analyzed by means of an iterative curve-fitting procedure (program Prism, GraphPad, San Diego, CA), which provided IC<sub>50</sub>, *K<sub>i</sub>*, and SEM values for tested compounds, the *K<sub>i</sub>* values being calculated from the Cheng and Prusoff equation.<sup>59</sup>

**Docking Calculations.** All the ligands were docked into the CBR model by means of Autodock 4.0 program. Docking simulations of the compounds were carried out by means of the Lamarckian genetic algorithm<sup>51</sup> and applying a protocol with an initial population of 50 randomly placed individuals, a maximum number of 1.0 × 10<sup>6</sup> energy evaluations, a mutation rate of 0.02, a crossover rate of 0.80, and an elitism value of 1. The pseudo Solis and Wets algorithm with a maximum of 300 interactions was applied for the local search. Then 100 independent docking runs were carried out for each ligand, and the resulting conformations that differ by less than 1.0 Å in positional root-mean-square deviation (rmsd) were clustered together. The conformer with the lowest free binding energy was taken as the representative of each cluster.

**Ligand Setup.** The structures of the ligands were generated by means of Discovery Studio software, version 1.5. Minimization energies were achieved by means of the CHARMM force field<sup>67</sup> as implemented in Discovery Studio. Minimization was carried out by means of 50 steps of steepest descent and 10 000 steps of conjugate gradient as minimization algorithms, with a rms convergence criterion of 0.01 Å. Partial atomic charges were assigned by means of the Gasteiger–Marsili formalism.<sup>68</sup> All the relevant torsion angles were treated as rotatable during the docking process, thus allowing a search of the conformational space.

**Protein Setup.** The GABA<sub>A</sub> receptor model was set up for docking as follows: polar hydrogens were added by means of Discovery Studio software, version 1.5, and Kollman united-atom partial charges were assigned. ADDSOL utility of the AutoDock program was used to add salvation parameters to the protein structures, and the grid maps representing the proteins in the docking process were calculated by means of AutoGrid. The grids, one for each atom type in the ligand plus

one for electrostatic interactions, were chosen to be large enough to include not only the hypothetical benzodiazepine binding site but also a significant part of the protein around it. As a consequence, for all docking calculations, the dimensions of grid map was  $46 \text{ \AA} \times 50 \text{ \AA} \times 56 \text{ \AA}$  with a grid-point spacing of  $0.375 \text{ \AA}$ .

**Energy Refinement of the CBR/Ligand Complexes.** The complexes obtained were subjected to energy minimization by means of CHARMM force field as implemented in Discovery Studio. Energy optimizations were carried out by means of 200 steps of steepest descent followed by 10 000 steps of conjugated gradient with an rms of 0.01 as gradient value.

**Molecular Electrostatic Potential Calculations.** For all compounds the electrostatic potential was calculated by means of Gaussian 03<sup>69</sup> and mapped onto the electron density surface for each compound. The isovalue of 0.0004 electron/bohr<sup>3</sup> was chosen for the definition of the density surface, while electrostatic potential was computed using Hartree–Fock functional and 6-31G\* basis set with a scale of  $-0.031$  (red) to  $0.031$  hartree (blue),  $-19.45$  and  $19.45 \text{ kcal mol}^{-1}$ , respectively.

**Molecular Dynamics Methods.** The pose representative of the most populated cluster for each compound (**5a**, **5f**, and **5j**) was used as starting point for further molecular dynamics simulations.

The binary complex between the benzodiazepine receptor and the ligand has been subjected to a molecular dynamics study, in explicit solvent and periodic boundary conditions, by means of NAMD2 molecular dynamics simulation code.<sup>70</sup> Protein and ligand were parametrized by using Xleap module of AMBER 9<sup>71</sup> in the parm99 version<sup>72</sup> of the all-atom AMBER force field.<sup>73,74</sup> The complex was subjected to the following procedure prior to molecular dynamics data collection: it was surrounded by a box of 6 Å layer of TIP3P31 pre-equilibrated water molecules<sup>75</sup> and neutralized by redistributing the net charge of the system equally on the backbone atoms of the proteins. A two-step preliminary minimization was carried out by using a sophisticated conjugate gradient and line search algorithm, first 2000 steps minimizing water, counterions, and hydrogens, then in the following 2000 steps the loops and all the side chains of the protein setting a convergence criterion on the gradient of  $0.0001 \text{ kcal mol}^{-1} \text{ \AA}^{-1}$ . The microcanonical NVE ensemble (constant volume and energy) was used to raise the system temperature to 300 K during 43 ps of Langevin dynamics simulations with starting  $5 \text{ kcal}/(\text{mol \AA}^2)$  restraints on protein backbone atoms and on the ligand heavy atoms, gradually decreased during the heating. The system was then equilibrated with respect to volume running for 70 ps until all the restraints were left off in NPT conditions (constant pressure and temperature) at 1 atm and 300 K using the Langevin dynamics to keep the temperature constant, while the pressure was controlled by using the Langevin piston Nose–Hoover method.<sup>76,77</sup> Eventually, the production run in the NPT ensemble was carried out.

van der Waals and short-range electrostatic interactions were estimated within a 10 Å cut-off with the switch value set to 8 Å and the pair list distance extended to 13.5 Å, whereas the long-range electrostatic interactions were assessed by using the particle mesh Ewald (PME) method,<sup>78</sup> with a grid size set to 120, 120, and 120 for *x*, *y* and *z* axes, respectively, and interpolated by a fourth-order function and by setting the direct sum tolerance to  $10^{-5}$ .

All the simulations of the solvated complex were performed with a time step of 2 fs in combination with the SHAKE<sup>79</sup> algorithm to constrain bond lengths involving hydrogen atoms.

The VMD program was used for visualization and data analysis.<sup>80</sup>

## ■ ASSOCIATED CONTENT

**Supporting Information.** Experimental details for the synthesis and characterization of intermediates **8e**, **i**, **9**, **10**, **13**, and **15–20**. This material is available free of charge via the Internet at <http://pubs.acs.org>.

## ■ AUTHOR INFORMATION

### Corresponding Author

\*For M.A.: phone, +39 577 234173; faxes +39 577 234333; e-mail, [anzini@unisi.it](mailto:anzini@unisi.it). For A.C.: phone, +39 577 234320; e-mail, [cappelli@unisi.it](mailto:cappelli@unisi.it).

## ■ ACKNOWLEDGMENT

We are grateful to Dr. Laura Salvini (C.I.A.D.S., University of Siena, Italy) for the recording of the mass spectra, to Prof. Stefania D'Agata D'Ottavi for the careful reading of the manuscript, and to INSTM (Consorzio Interuniversitario Nazionale per la Scienza e la Tecnologia dei Materiali) for the access to Accelrys software. We are also grateful to Prof. Cromer for kindly providing us with the homology model of the GABA<sub>A</sub> receptor. This work was financially supported by CNR (Consiglio Nazionale delle Ricerche) and MIUR (Ministero dell'Università e della Ricerca), PRIN (Programmi di Ricerca di Rilevante Interesse Nazionale).

## ■ DEDICATION

†In honor of the 80th birthday of R. Ian Fryer, Professor Emeritus of Medicinal Chemistry at the Department of Chemistry, Rutgers The State University of New Jersey, Newark, New Jersey 07102, United States.

## ■ ABBREVIATIONS USED

CBR, central benzodiazepine receptor; BDZ, benzodiazepine; GABA,  $\gamma$ -aminobutyric acid; CNS, central nervous system; GR,  $\gamma$ -aminobutyric acid ratio; CMC, carboxymethylcellulose; DZ, diazepam; MD, molecular dynamics; SAR, structure–activity relationship; rmsd, root-mean-square deviation; IBDZ, imidazo-benzodiazepine

## ■ REFERENCES

- (1) Sieghart, W. Structure and Pharmacology of Gamma-Aminobutyric Acid A Receptor Subtypes. *Pharmacol. Rev.* **1994**, *47*, 181–234.
- (2) Smith, G. B.; Olsen, R. W. Functional Domains of GABA<sub>A</sub> Receptors. *Trends Pharmacol. Sci.* **1995**, *16*, 162–168.
- (3) Argyropoulos, S. V.; Nutt, D. J. The Use of Benzodiazepines in Anxiety and Other Disorders. *Eur. Neuropsychopharmacol.* **1999**, *9*, 391–392.
- (4) Park-Chung, M.; Malayev, A.; Purdy, R. H.; Gibbs, T. T.; Farb, D. H. Sulfated and Unsulfated Steroids Modulate  $\gamma$ -Aminobutyric Acid Receptor A Function through Distinct Sites. *Brain Res.* **1999**, *830*, 72–87.
- (5) Rupperecht, R.; Holsboer, F. Neuroactive Steroids: Mechanisms of Action and Neuropsychopharmacological Perspectives. *Trends Neurosci.* **1999**, *22*, 410–416.
- (6) Dorow, R. FG7142 and Its Anxiety Inducing Effects in Humans. *Br. J. Clin. Pharmacol.* **1987**, *23*, 781–782.
- (7) Williams, T. J.; Bowie, P. E. Midazolam Sedation To Produce Complete Amnesia for Bronchoscopy: 2 Years' Experience at a District General Hospital. *Respir. Med.* **1999**, *93*, 361–365.
- (8) Stewart, S. A. The Effects of Benzodiazepines on Cognition. *J. Clin. Psychiatry* **2005**, *66*, 9–13.
- (9) Lister, R. G. The Amnestic Action of Benzodiazepines in Man. *Neurosci. Biobehav. Rev.* **1985**, *9*, 87–94.
- (10) Ghoneim, M. M.; Mewaldt, S. P. Benzodiazepines and Human Memory: A Review. *Anesthesiology* **1990**, *72*, 926–938.
- (11) Chambers, M. S.; Attack, J. R.; Broughton, H. B.; Collinson, N.; Cook, S.; Dawson, G. R.; Hobbs, S. C.; Marshall, G.; Maubach, K. A.

Pillai, G. V.; Reeve, A. J.; MacLeod, A. M. Identification of a Novel, Selective GABA<sub>A</sub>  $\alpha_5$  Receptor Inverse Agonist Which Enhances Cognition. *J. Med. Chem.* **2003**, *46*, 2227–2240.

(12) Sarter, M.; Bruno, J. P.; Berntson, G. G. Psychotogenic Properties of Benzodiazepine Receptor Inverse Agonists. *Psychopharmacology* **2001**, *156*, 1–13.

(13) Wolkowitz, O. M.; Reus, V. I.; Roberts, E.; Manfredi, F.; Chan, T.; Ormiston, R.; Johnson, J.; Canick, J.; Brizendine, H.; Weingartner, H. Antidepressant and Cognition-Enhancing Effects of DHEA in Major Depression. *Ann. N.Y. Acad. Sci.* **1995**, *774*, 337–339.

(14) Bloch, M.; Schmidt, P. J.; Danaceau, M. A.; Adams, L. F.; Rubinow, D. R. Dehydroepiandrosterone Treatment of Midlife Dysthymia. *Biol. Psychiatry* **1999**, *45*, 1533–1541.

(15) Wolf, O. T.; Köster, B.; Kirschbaum, C.; Pietrowsky, R.; Kern, W.; Hellhammer, D. H.; Born, J.; Fehm, H. L. A Single Administration of Dehydroepiandrosterone Does Not Enhance Memory Performance in Young Healthy Adults, but Immediately Reduces Cortisol Levels. *Biol. Psychiatry* **1997**, *42*, 845–848.

(16) Vallée, M.; Mayo, W.; Le Moal, M. Role of Pregnenolone, Dehydroepiandrosterone and Their Sulfate Esters on Learning and Memory in Cognitive Aging. *Brain Res. Rev.* **2001**, *37*, 301–312.

(17) Dorow, R.; Horowski, R.; Paschelke, G.; Amin, M.; Braestrup, C. Severe Anxiety Induced by FG 7142, a  $\beta$ -Carboline Ligand for Benzodiazepine Receptors. *Lancet* **1983**, *322*, 98–99.

(18) Knoflach, F.; Rhyner, Th.; Villa, M.; Kellenberger, S.; Drescher, U.; Malherbe, P.; Sigel, E.; Mohler, H. The  $\gamma$ 3-Subunit of the GABA<sub>A</sub>-Receptor Confers Sensitivity to Benzodiazepine Receptor Ligands. *FEBS Lett.* **1991**, *293*, 191–194.

(19) Barnard, E. A.; Skolnick, P.; Olsen, R. W.; Molhler, H.; Sieghart, W.; Biggio, G.; Braestrup, C.; Bateson, A. N.; Langer, S. Z. International Union of Pharmacology. XV. Subtypes of  $\gamma$ -Aminobutyric Acid A Receptors: Classification on the Basis of Subunit Structure and Receptor Function. *Pharmacol. Rev.* **1998**, *50*, 291–313.

(20) Ernst, M.; Brauchart, D.; Boresch, S.; Sieghart, W. Comparative Modeling of GABA-A Receptor: Limits, Insights, Future Developments. *Neuroscience* **2003**, *119*, 933–943.

(21) McKernan, R. M.; Rosahl, T. W.; Reynolds, D. S.; Sur, C.; Wafford, K. A.; Attack, J. R.; Farrar, S.; Myers, J.; Cook, G.; Ferris, P.; Garrett, L.; Bristow, L.; Marshall, G.; Macaulay, A.; Brown, N.; Howell, O.; Moore, K. W.; Carling, R. W.; Street, L. J.; Castro, J. L.; Ragan, C. I.; Dawson, G. R.; Whiting, P. J. Sedative but Not Anxiolytic Properties of Benzodiazepines Are Mediated by the GABA<sub>A</sub> Receptor  $\alpha$ 1 Subtype. *Nat. Neurosci.* **2000**, *3*, 587–592.

(22) Rudolph, U.; Möhler, H. Analysis of GABA<sub>A</sub> Receptor Function and Dissection of the Pharmacology of Benzodiazepines and General Anaesthetics through Mouse Genetics. *Annu. Rev. Pharmacol. Toxicol.* **2004**, *44*, 475–498.

(23) Attack, J. R.; Hutson, P. H.; Collinson, N.; Marshall, G.; Bentley, G.; Moyes, C.; Cook, S. M.; Collins, I.; Wafford, K.; McKernan, R. M.; Dawson, G. R. Anxiogenic Properties of an Inverse Agonist Selective for  $\alpha$ 3 Subunit-containing GABA<sub>A</sub> Receptors. *Br. J. Pharmacol.* **2005**, *144*, 357–366.

(24) Wisden, W.; Laurie, D. J.; Monyer, H.; Seeburg, P. H. The Distribution of 13 GABA<sub>A</sub> Receptor Subunit mRNAs in the Rat Brain. I. Telencephalon, Diencephalon, Mesencephalon. *J. Neurosci.* **1992**, *12*, 1040–1062.

(25) Thompson, C. L.; Bodewitz, G.; Stephenson, F. A.; Turner, J. D. Mapping of GABA<sub>A</sub> Receptor  $\alpha$ 5 and  $\alpha$ 6 Subunit-like Immunoreactivity in Rat Brain. *Neurosci. Lett.* **1992**, *144*, 53–56.

(26) Brünig, I.; Scotti, E.; Sidler, C. Intact Sorting, Targeting, and Clustering of Gamma-Butyric Acid Receptor Subtypes in Hippocampal Neurons in Vitro. *J. Comp. Neurol.* **2002**, *443*, 43–55.

(27) Caraiscos, V. B.; Elliott, E. M.; You-Ten, K. E.; Cheng, V. Y.; Belelli, D.; Newell, J. G.; Jackson, M. F.; Lambert, J. J.; Rosahl, T. W.; Wafford, K. A.; MacDonald, J. F.; Orser, B. A. Tonic Inhibition in Mouse Hippocampal CA1 Pyramidal Neurons Is Mediated by  $\alpha$ 5 Subunit-Containing  $\gamma$ -Aminobutyric Acid Type A Receptors. *Proc. Natl. Acad. Sci. U.S.A.* **2004**, *101*, 3662–3667.

(28) Caraiscos, V. B.; Newell, J. G.; You-Ten, K. E.; Elliott, E. M.; Rosahl, T. W.; Wafford, K. A.; MacDonald, J. F.; Orser, B. A. Selective Enhancement of Tonic GABAergic Inhibition in Murine Hippocampal Neurons by Low Concentrations of the Volatile Anesthetic Isoflurane. *J. Neurosci.* **2004**, *24*, 8454–8458.

(29) Gilman, S.; Newman, S. The Hypothalamus and Limbic System. In *Essentials of Clinical Neuroanatomy and Neurophysiology*; Manter, J., Gatz, A., Eds.; Davis: Philadelphia, PA, 1992; pp 219–225.

(30) McNaughton, N.; Morris, R. G. M. Chlordiazepoxide, an Anxiolytic Benzodiazepine, Impairs Place Navigation in Rats. *Behav. Brain Res.* **1991**, *24*, 39–46.

(31) Maubach, K. GABA<sub>A</sub> Receptor Subtype Selective Cognition Enhancers. *Curr. Drug Targets: CNS Neurol. Disord.* **2003**, *2*, 233–239.

(32) Carling, R. W.; Moore, K. W.; Street, L. J.; Wild, D.; Isted, C.; Leeson, P. D.; Thomas, S.; O'Connor, D.; McKernan, R. M.; Quirk, K.; Cook, S. M.; Attack, J. R.; Wafford, K. A.; Thompson, S. A.; Dawson, G. R.; Ferris, P.; Castro, J. L. 3-Phenyl-6-(2-pyridyl)methoxy-1,2,4-triazolo[3,4-a]phthalazines and Analogues: High-Affinity  $\gamma$ -Aminobutyric Acid-A Benzodiazepine Receptor Ligands with  $\alpha$ 2,  $\alpha$ 3, and  $\alpha$ 5-Subtype Binding Selectivity Over  $\alpha$ 1. *J. Med. Chem.* **2004**, *47*, 1807–1822.

(33) Huang, Q.; He, X.; Ma, C.; Liu, R.; Yu, S.; Dayer, C. A.; Wenger, G. R.; McKernan, R.; Cook, J. M. Pharmacophore/Receptor Models for GABA<sub>A</sub>/BzR Subtypes ( $\alpha$ 1 $\beta$ 3 $\gamma$ 2,  $\alpha$ 5 $\beta$ 3 $\gamma$ 2, and  $\alpha$ 6 $\beta$ 3 $\gamma$ 2) via a Comprehensive Ligand-Mapping Approach. *J. Med. Chem.* **2000**, *43*, 71–95.

(34) Liu, R.; Hu, R. J.; Zhang, P.; Skolnick, P.; Cook, J. M. Synthesis and Pharmacological Properties of Novel 8-Substituted Imidazobenzodiazepines: High-Affinity, Selective Probes for  $\alpha$ 5-Containing GABA<sub>A</sub> receptors. *J. Med. Chem.* **1996**, *39*, 1928–1934.

(35) Liu, R.; Zhang, P.; McKernan, R. M.; Wafford, K.; Cook, J. M. Synthesis of Novel Imidazobenzodiazepines Selective for the  $\alpha$ 5 $\beta$ 2 $\gamma$ 2 (Bz5)/Benzodiazepine Receptor Subtype. *Med. Chem. Res.* **1995**, *5*, 700–709.

(36) Harris, D.; Clayton, T.; Cook, J.; Sahbaie, P.; Halliwell, R. F.; Furtmüller, R.; Huck, S.; Sieghart, W.; DeLorey, T. M. Selective Influence on Contextual Memory: Physicochemical Properties Associated with Selectivity of Benzodiazepine Ligands at GABA<sub>A</sub> Receptors Containing the  $\alpha$ 5 Subunit. *J. Med. Chem.* **2008**, *51*, 3788–3803.

(37) Anzini, M.; Braile, C.; Valenti, S.; Cappelli, A.; Vomero, S.; Marinelli, L.; Limongelli, V.; Novellino, E.; Betti, L.; Giannaccini, G.; Lucacchini, A.; Ghelardini, C.; Galeotti, N.; Makovec, F.; Giorgi, G.; Fryer, R. I. Ethyl 8-Fluoro-6-(3-nitrophenyl)-4H-imidazo[1,5-a][1,4]benzodiazepine-3-carboxylate as Novel, Highly Potent and Safe Antianxiety Agent. *J. Med. Chem.* **2008**, *51*, 4730–4743.

(38) Fryer, R. I.; Gu, Z. Q.; Wang, C. G. Synthesis of Novel, Substituted 4H-Imidazo[1,5-a][1,4]benzodiazepine. *J. Heterocycl. Chem.* **1991**, *28*, 1661–1669.

(39) Walsh, D. A. The Synthesis of 2-Aminobenzophenones. *Synthesis* **1980**, *32*, 677–688.

(40) Walser, A.; Fryer, R. I. Bicyclic Diazepines, Chapter VII: Dihydro-1,4-benzodiazepinones and Thiones. In *The Chemistry of Heterocyclic Compounds*; Fryer, R. I., Ed.; John Wiley & Sons Inc.: New York, 1991; Vol. 50, pp 713–836 and references therein.

(41) Zhang, W.; Koehler, K. F.; Harris, B.; Skolnick, P.; Cook, J. C. Synthesis of Benzo-Fused Benzodiazepines Employed as Probes of the Agonist Pharmacophore of Benzodiazepine Receptors. *J. Med. Chem.* **1994**, *37*, 745–757.

(42) Okabe, M.; Chu, S. R.; Tam, S. Y. K.; Todaro, L. J.; Coffen, D. L. Synthesis of the Dideoxynucleosides “ddC” and “CNT” from Glutamic Acid, Ribonolactone, and Pyrimidine Bases. *J. Org. Chem.* **1988**, *53*, 4780–4786.

(43) Braestrup, C.; Nielsen, M.; Honoré, T.; Jensen, L. H.; Petersen, E. N. Benzodiazepine Receptor Ligands with Positive and Negative Efficacy. *Neuropharmacology* **1983**, *22*, 1451–1457.

(44) Braestrup, C.; Nielsen, M. Benzodiazepine Receptors. In *Handbook of Psychopharmacology*; Iversen, L. L., Iversen, S. D., Snyder, S. H., Eds.; Plenum Press: New York, 1983; Vol. 17, pp 285–384.

(45) Fryer, R. I.; Rios, R.; Zhang, P.; Gu, Z. Q.; Basile, A. S.; Skolnick, P. Structure–Activity Relationships of 2-Pyrazolo[4,3-c]quinoline-3-ones

and Their *N*- and *O*-Methyl Analogues at Benzodiazepine Receptors. *Med. Chem. Res.* **1993**, *3*, 122–130.

(46) Fryer, R. I. Ligand Interactions at Central Benzodiazepine Receptor. In *Comprehensive Medicinal Chemistry*; Hansch, C., Sammes, P. G., Taylor, J. B., Eds; Pergamon: Oxford, U.K., 1990; Vol. 3, pp 539–566.

(47) Schwartz, R. D.; Suzdak, P. D.; Paul, S. M.  $\alpha$ -Aminobutyric Acid (GABA)- and Barbiturate-Mediated  $^{36}\text{Cl}^-$  Uptake in Rat Brain Synaptoneuroosomes: Evidence for Rapid Desensitization of the GABA Receptor-Coupled Chloride Ion Channel. *Mol. Pharmacol.* **1986**, *30*, 419–426.

(48) Im, H. K.; Im, W. B.; Hamilton, B. J.; Carter, D. B.; VonVoigtlander, P. F. Potentiation of GABA-Induced Chloride Currents by Various Benzodiazepine Site Agonists with  $\alpha_1\gamma_2$ ,  $\beta_2\gamma_2$  and  $\alpha_1\beta_2\gamma_2$  Subtypes of Cloned GABA<sub>A</sub> Receptors. *Mol. Pharmacol.* **1993**, *44*, 866–870.

(49) Möhler, H.; Fritschy, J. M.; Rudolph, U. A New Benzodiazepine Pharmacology. *J. Pharmacol. Exp. Ther.* **2002**, *300*, 2–8.

(50) (a) Cromer, B. A.; Morton, J. C.; Parker, M. W. Anxiety over GABA<sub>A</sub> Receptor Structure Relieved by AChBP. *Trends Biochem. Sci.* **2002**, *27*, 280–287. (b) Ernst, M.; Brauchart, D.; Boresch, S.; Sieghart, W. Comparative Modeling of GABA(A) Receptors: Limits, Insights, Future Developments. *Neuroscience* **2003**, *119*, 933–943.

(51) Morris, G. M.; Goodsell, D. S.; Halliday, R. S.; Huey, R.; Hart, W. E.; Belew, R. K.; Olson, A. J. Automated Docking Using a Lamarckian Genetic Algorithm and Empirical Binding Free Energy Function. *J. Comput. Chem.* **1998**, *19*, 1639–1662.

(52) (a) Saraogi, I.; Vijay, V. G.; Das, S.; Sekar, K.; Guru Row, T. N. C–Halogen  $\cdots\pi$  Interactions in Proteins: a Database Study. *Cryst. Eng.* **2003**, *6*, 69–77. (b) Kahnberg, P.; Lager, E.; Rosenberg, C.; Schougaard, J.; Camet, L.; Sterner, O.; Nielsen, E.; Nielsen, M.; Liljefors, T. Refinement and Evaluation of a Pharmacophore Model for Flavone Derivatives Binding to the Benzodiazepine Site of the GABA<sub>A</sub> Receptor. *J. Med. Chem.* **2002**, *45*, 4188–4201.

(53) Sheldrick, G. M. *SHELXS-97: A Program for Automatic Solution of Crystal Structures*, release 97-2; Göttingen University: Göttingen, Germany, 1997.

(54) Sheldrick, G. M. *SHELXL-97: A Program for Crystal Structure Refinement*, release 97-2; Göttingen University: Göttingen, Germany, 1997.

(55) Martini, C.; Lucacchini, A.; Ronca, G.; Hrelia, S.; Rossi, C. A. Isolation of Putative Benzodiazepine Receptors from Rat Brain Membranes by Affinity Chromatography. *J. Neurochem.* **1982**, *38*, 15–19.

(56) Martini, C.; Rigacci, T.; Lucacchini, A. [ $^3\text{H}$ ]Muscimol Binding Site on Purified Benzodiazepine Receptor. *J. Neurochem.* **1983**, *41*, 1183–1185.

(57) Lowry, O. H.; Rosenbrouh, N. J.; Farr, A. L.; Randall, R. J. Protein Measurement with the Folin Phenol Reagent. *J. Biol. Chem.* **1951**, *193*, 265–275.

(58) Bertelli, L.; Biagi, G.; Giorgi, I.; Manera, C.; Livi, O.; Scartoni, V.; Betti, L.; Giannaccini, G.; Trincavelli, L.; Barili, P. L. 1,2,3-Triazololo-[1,5-*a*]quinoxalines: Synthesis and Binding to Benzodiazepine and Adenosine Receptors. *Eur. J. Med. Chem.* **1998**, *33*, 113–122.

(59) Cheng, Y. C.; Prusoff, W. H. Relationship Between the Inhibition Constant ( $K_i$ ) and the Concentration of Inhibition Which Causes 50 Percent Inhibition ( $\text{IC}_{50}$ ) of an Enzyme Reaction. *Biochem. Pharmacol.* **1973**, *22*, 3099–3108.

(60) Vaught, J.; Pelley, K.; Costa, L. G.; Setler, P.; Enna, S. J. A Comparison of the Antinociceptive Responses to GABA-Receptor Agonist THIP and Baclofen. *Neuropharmacology* **1985**, *4*, 211–216.

(61) Walsh, D. M.; Stratton, S. C.; Harvey, F. J.; Beresford, I. J.; Hagan, R. M. The Anxiolytic-like Activity of GR159897, a Non-Peptide NK2 Receptor Antagonist, in Rodent and Primate Models of Anxiety. *Psychopharmacology* **1995**, *122*, 186–191.

(62) Jarvik, M. E.; Kopp, R. An Improved One-Trial Passive Avoidance Learning Situation. *Psychol. Rep.* **1967**, *21*, 221–224.

(63) Guerrini, G.; Costanzo, A.; Ciciani, G.; Bruni, F.; Selleri, S.; Costagli, C.; Besnard, F.; Costa, B.; Martini, C.; De Siena, G.;

Malmberg-Aiello, P. Benzodiazepine Receptor Ligands. 8: Synthesis and Pharmacological Evaluation of New Pyrazolo[5,1-*c*][1,2,4]benzotriazine-5-oxide 3- and 8-Disubstituted: High Affinity Ligands Endowed with Inverse-Agonist Pharmacological Efficacy. *Bioorg. Med. Chem.* **2006**, *14*, 758–775.

(64) Mascia, M. P.; Machu, T. K.; Harris, R. A. Enhancement of Homomeric Glycine Receptor Function by Long-Chain Alcohols and Anaesthetics. *Br. J. Pharmacol.* **1996**, *119*, 1331–1336.

(65) Colman, A. Expression of Exogenous DNA in *Xenopus* Oocytes. In *Transcription and Translation: A Practical Approach*; Hames, B. D., Higgins, S. J., Eds.; Oxford Press: Washington, DC, 1984; pp 49–59.

(66) Besnard, F.; Even, Y.; Itier, V.; Granger, P.; Partiseti, M.; Avenet, P.; Depoortere, H.; Graham, D. Development of Stable Cell Lines Expressing Different Subtypes of GABA<sub>A</sub> Receptors. *J. Recept. Signal Transduction Res.* **1997**, *17*, 99–113.

(67) Brooks, B. R.; Bruccoleri, R. E.; Olafson, D. B.; States, D. J.; Swaminathan, S.; Karplus, M. CHARMM: A Program for Macromolecular Energy, Minimization and Dynamics Calculations. *J. Comput. Chem.* **1983**, *4*, 187–217.

(68) Gasteiger, J.; Marsili, M. Iterative Partial Equalization of Orbital Electronegativity: A Rapid Access to Atomic Charges. *Tetrahedron* **1980**, *36*, 3219–3228.

(69) Frisch, M. J.; Trucks, G. W.; Schlegel, H. B.; Scuseria, G. E.; Robb, M. A.; Cheeseman, J. R.; Montgomery, J. A., Jr.; Vreven, T.; Kudin, K. N.; Burant, J. C.; Millam, J. M.; Iyengar, S. S.; Tomasi, J.; Barone, V.; Mennucci, B.; Cossi, M.; Scalmani, G.; Rega, N.; Petersson, G. A.; Nakatsuji, H.; Hada, M.; Ehara, M.; Toyota, K.; Fukuda, R.; Hasegawa, J.; Ishida, M.; Nakajima, T.; Honda, Y.; Kitao, O.; Nakai, H.; Klene, M.; Li, X.; Knox, J. E.; Hratchian, H. P.; Cross, J. B.; Bakken, V.; Adamo, C.; Jaramillo, J.; Gomperts, R.; Stratmann, R. E.; Yazyev, O.; Austin, A. J.; Cammi, R.; Pomelli, C.; Ochterski, J. W.; Ayala, P. Y.; Morokuma, K.; Voth, G. A.; Salvador, P.; Dannenberg, J. J.; Zakrzewski, V. G.; Dapprich, S.; Daniels, A. D.; Strain, M. C.; Farkas, O.; Malick, D. K.; Rabuck, A. D.; Raghavachari, K.; Foresman, J. B.; Ortiz, J. V.; Cui, Q.; Baboul, A. G.; Clifford, S.; Cioslowski, J.; Stefanov, B. B.; Liu, G.; Liashenko, A.; Piskorz, P.; Komaromi, I.; Martin, R. L.; Fox, D. J.; Keith, T.; Al-Laham, M. A.; Peng, C. Y.; Nanayakkara, A.; Challacombe, M.; Gill, P. M. W.; Johnson, B.; Chen, W.; Wong, M. W.; Gonzalez, C.; Pople, J. A. *Gaussian 03*, revision C.02; Gaussian, Inc.: Wallingford, CT, 2004.

(70) Phillips, J. C.; Braun, R.; Wang, W.; Gumbart, J.; Tajkhorshid, E.; Villa, E.; Chipot, C.; Skeel, R. D.; Kale, L.; Schulten, K. Scalable Molecular Dynamics with NAMD. *J. Comput. Chem.* **2005**, *26*, 1781–1802.

(71) Case, D. A.; Darden, T. A.; Cheatham, T. E., III; Simmerling, C. L.; Wang, J.; Duke, R. E.; Luo, R.; Merz, K. M.; Pearlman, D. A.; Crowley, M.; Walker, R. C.; Zhang, W.; Wang, B.; Hayik, S.; Roitberg, A.; Seabra, G.; Wong, K. F.; Paesani, F.; Wu, X.; Brozell, S.; Tsui, V.; Gohlke, H.; Yang, L.; Tan, C.; Mongan, J.; Hornak, V.; Cui, G.; Beroza, P.; Mathews, D. H.; Schafmeister, C.; Ross, W. S.; Kollman, P. A. *AMBER 9*; University of California: San Francisco, CA, 2006.

(72) Wang, J.; Cieplak, P.; Kollman, P. A. How Well Does a Restrained Electrostatic Potential (RESP) Model Perform in Calculating Conformational Energies of Organic and Biological Molecules? *J. Comput. Chem.* **2000**, *21*, 1049–1074.

(73) Cornell, W. D.; Cieplak, P.; Bayly, C. I.; Gould, I. R.; Merz, K. M.; Ferguson, D. M.; Spellmeyer, D. C.; Fox, T.; Caldwell, J. W.; Kollman, P. A. A Second Generation Force Field for the Simulation of Proteins, Nucleic Acids, and Organic Molecules. *J. Am. Chem. Soc.* **1995**, *117*, 5179–5197.

(74) Hornak, V.; Abel, R.; Okur, A.; Strockbine, B.; Roitberg, A.; Simmerling, C. Comparison of Multiple Amber Force Fields and Development of Improved Protein Backbone Parameters. *Proteins* **2006**, *65*, 712–725.

(75) Jorgensen, W. L.; Chandrasekhar, J.; Madura, J. D.; Impey, R. W.; Klein, L. M. Comparison of Simple Potential Functions for Simulating Liquid Water. *J. Chem. Phys.* **1983**, *79*, 926–935.

- (76) Martyna, G. J.; Tobias, D. J.; Klein, M. L. Constant Pressure Molecular Dynamics Algorithms. *J. Chem. Phys.* **1994**, *101*, 4177–4189.
- (77) Feller, S. E.; Zhang, Y.; Pastor, R. W.; Brooks, B. R. Constant Pressure Molecular Dynamics Simulation: The Langevin Piston Method. *J. Chem. Phys.* **1995**, *103*, 4613–4621.
- (78) Essmann, U.; Perera, L.; Berkowitz, M. L.; Darden, T.; Lee, H.; Pedersen, L. G. A Smooth Particle Mesh Ewald Method. *J. Chem. Phys.* **1995**, *103*, 8577–8593.
- (79) Ryckaert, J. P.; Ciccotti, G.; Berendsen, H. J. C. Numerical Integration of the Cartesian Equations of Motion of a System with Constraints: Molecular Dynamics of *n*-Alkanes. *J. Comput. Phys.* **1977**, *23*, 327–341.
- (80) Humphrey, W.; Dalke, A.; Schulten, K. Visual Molecular Dynamics. *J. Mol. Graphics* **1996**, *14*, 33–38.